NTNU – Trondheim
Norwegian University of
Science and Technology

Testing of Fibre Reinforced Concrete Structures

Structural Behaviour in the Serviceability and Ultimate Limit States

Øystein Flakk
Kristian Nesse Tordal

Civil and Environmental Engineering (2 year)
Submission date: June 2012
Supervisor: Terje Kanstad, KT
Co-supervisor: Giedrius Zingulis, KT
Elena Sarmiento, KT

Norwegian University of Science and Technology
Department of Structural Engineering

Department of Structural Engineering
Faculty of Engineering Science and Technology
NTNU- Norwegian University of Science and Technology

ACCESSIBILITY

OPEN

MASTER THESIS 2012

SUBJECT AREA:	DATE:	NO. OF PAGES:
Concrete Structures	09.06.2012	91 pages + 4 appendix + CD

TITLE:

Testing of fibre reinforced concrete structures: Structural behaviour in the Serviceability and Ultimate limit states

Prøving av fiberarmerte betongkonstruksjoner:
Konstruksjonsoppførsel I bruks- og bruddgrensetilstanden

BY:

Kristian Nesse Tordal

Øystein Flakk

SUMMARY:

This master's thesis contains studies on moment capacity of fibre reinforced concrete in load-bearing structures. The primary focus has been testing of full scale beams with steel fibres, both with and without additional reinforcing bars. The properties of both the fresh and hardened concrete have also been studied and measured in accordance with current standards and regulations.

The concrete used in the experiments was self compacting with a fibre content of 80 kg/m^3 corresponding to 1 vol-% of the concrete.

In addition to laboratory experiments, calculations were performed according to current guidelines for design of fibre reinforced structures to estimate the expected behaviour of the beams.

The thesis also includes literature study focusing on the use of fibres in concrete, material composition, moment capacity and crack development of fibre reinforced concrete.

RESPONSIBLE TEACHER: Terje Kanstad

SUPERVISORS: Elena Vidal Sarmiento and Giedrius Zirgulis

CARRIED OUT AT: Department of structural engineering

NORGES TEKNISK NATURVITENSKAPELIGE
UNIVERSITET, NTNU
Institutt for konstruksjonsteknikk

Master-oppgave i konstruksjonsteknikk VÅREN 2012

for

Øystein Flakk og Kristian Nesse Tordal

Prøving av fiberarmerte betongkonstruksjoner: Konstruksjonsoppførsel i bruks- og bruddgrensetilstanden

Testing of fibre reinforced concrete structures: Structural behaviour in the Serviceability and Ultimate limit states

INTRODUCTION

Fibre reinforcement replacing ordinary reinforcing bars is very interesting today due to economical reasons, need for rationalisation, and improved work conditions in the building and construction industry. The R&D activity internationally and in Norway has increased the last years and new types of fibres have been available at the markets. Furthermore, several international pre-normative regulations have also been launched, and a proposal for Norwegian guidelines has been published.

This MSc thesis is connected to the research programme COIN, which is a centre for research and innovation financed by the Norwegian Research council, the concrete industry through active partners. Sintef and NTNU, Department of structural engineering are the research partners in this project.

The principal aim of this Master's thesis is to use fibre reinforcement as a substitute for conventional bar reinforcement in bending problems, and the main focus is on crack distribution, crack widths and moment capacity.

COURSE

The thesis includes a literature study which shall include relevant theory, and alternative design methods and guidelines.

The experimental part shall include testing of fibre reinforced beams made of flowable concrete.

The evaluation of the results shall be related to current design methods, guidelines and previous results, and the capacity, ductility, cracking load and crack pattern shall be investigated.

GENERELT

Supervisors: Terje Kanstad, Elena Vidal Sarmiento and Giedrius Zirgulis.

The MSC thesis shall be finished within June 11th 2012.

Trondheim den 06.06.2012

Terje Kanstad
Professor

Foreword

This report concludes our 2-year master's programme at NTNU in Trondheim. The report exhibit the work we have conducted during the last semester.

The assignment was a mixture of practical experiments and theoretical studies within a very interesting research field, fibre reinforced concrete. The main reason for this choice of master thesis was the opportunity given to work with full scale structural parts in practice. Laboratory testing and literature studies have raised our theoretical knowledge and understanding in the field of concrete.

We would like to thank our main supervisor Terje Kanstad for all help during the work with this thesis. Also the supervision and assistance from Giedrius Zirgulis, Elena Vidal Sarmiento and Maria Belen Fernadez are greatly appreciated.

Thanks to the laboratory engineers, Steinar Seehuus, Ove Loraas, Gøran Loraas and Ragnar Moen, for help with casting and testing of our full scale test beams.

NTNU, Trondheim, June 2012

Kristian Nesse Tordal

Øystein Flakk

Abstract

This master's thesis contains studies on moment capacity of fibre reinforced concrete in load-bearing structures. The primary focus has been testing of full scale beams with steel fibres, both with and without additional reinforcing bars. The beams were tested in a 4-point bending test and the behaviour of the beams was monitored during testing. The properties of both the fresh and hardened concrete have also been studied and measured in accordance with current standards and regulations.

The fibres tensile strength contribution has been determined by testing of standard beams as described in NS-EN 14651. In this test, a residual flexural tensile strength was calculated based on monitored deflection and crack widths. The compressive strength of the concrete was determined by testing of standard cubes.

The concrete used in the experiments was a self compacting concrete proportioned as B35 and the fibre reinforcement type was Dramix 65/60. The amount of fibres was 1 vol-%, equivalent to 80 kg per cubic meter of concrete.

In addition to laboratory experiments, calculations were performed according to current guidelines for design of fibre reinforced structures to estimate the expected behaviour of the beams. The calculations have been compared to the results from beam testing for evaluation.

The thesis also includes literature study focusing on the use of fibres in concrete, material composition, moment capacity and crack development of fibre reinforced concrete.

The results from the testing show that fibre reinforcement has a significant effect on the moment capacity, and that steel fibres in many cases can meet the requirements in serviceability state without additional reinforcing bars. The steel fibre amount of 1 vol% gave higher moment capacity than expected based on calculations made prior to the testing. Observations and measurements made during testing, also show that the fibres have a favourable effect on the crack development by limiting crack widths and ensuring an evenly distributed crack pattern before the main crack occurs.

Sammendrag

Denne masteroppgaven inneholder studier gjort på momentkapasitet av stålfiberarmert betong i bærende konstruksjoner. Hovedfokuset har vært laboratorietesting av fullskala bjelker, med og uten konvensjonell armering i tillegg til stålfiberarmering. Bjelkene ble testet i en fire punkts bøyetest og bjelkenes oppførsel ble målt underveis i testingen. Betongens egenskaper, både i fersk og herdet tilstand, har også blitt undersøkt og dokumentert i henhold til gjeldende regler og standardverk.

Fiberbidraget til betongens strekkstyrke har blitt bestemt ved bruk av en standardbjelketest utført etter NS-EN 14651. Der blir referansebjelker testet og rest bøyestrekkfastet beregnet ut ifra et forhold mellom nedbøyning og målte rissvidder. Betongens trykkfasthet har blitt bestemt ved trykktesting av terninger.

Betongen brukt i denne oppgaven var en selvkomprimerende betong planlagt til å være av B35 kvalitet. Fiberarmeringen som ble brukt var stålfiber av typen Dramix 65/60. Mengden stålfiber brukt til testbjelkene var 1 vol-% av betongen, noe som tilsvarer 80 kg fiber per kubikkmeter betong.

I tillegg til laboratorieforsøk er det utført bergeninger for bjelkene ut i fra forslag til retningslinjer for dimensjonering av fiberarmert betong. Beregningen har blitt sammenlignet med resultatene fra bjelketestingen for å vurdere resultatene.

Rapporten inneholder også et litteraturstudie med fokus på bruk av fiber i betong, materialsammensetning av fiberbetong, momentkapasitet av fiberarmert betong og rissutvikling i fiberarmert betong.

Resultatene i denne oppgaven viser at fiberarmering har en betydelig effekt på momentkapasiteten, og at stålfiber i mange tilfeller kan tilfredsstille kravene i bruksgrense uten bruk av stangarmering. Stålfiberinnholdet på 1 vol-% brukt i denne oppgaven ga høyere momentkapasitet enn forventet ut ifra beregninger gjort på forhånd. Observasjoner og målinger gjort under testing av fullskala bjelkene viser at stålfiberene har en gunstig virkning på rissforløpet, ved at rissviddene reduseres og at det dannes et jevnt fordelt mønster av små riss før hovedrisset oppstår.

Contents

List of Figures

List of Tables

Part I

Literature study

1 Fibre reinforced concrete

1.1 Use of fibre reinforced concrete

Concrete as construction material has a very good ability to withstand compressive forces, but it can not withstand tensile loading to the same extent. It is necessary to enhance the tensile zone in concrete if it is to be used in load bearing constructions. Steel rods (rebars) are commonly used as reinforcement in concrete. The tensile forces in the concrete are transferred from the concrete to the rebars when the tensile capacity of the concrete is depleted and cracks occur. The forces are transmitted through the bond between the concrete and the rebars. One of the main issues with rebars is the time consuming process of designing the rebar layout and placing the rebars before casting.

Steel fibres as a replacement for regular rebar reinforcement will make the casting process easier and much faster, especially combined with self compacting concrete. The fibres can be added directly in the concrete mix at a mixing-plant or in a "Auto-mixer" at the construction site.

Regular rebar reinforcement is exposed to corrosion, and the only protection against corrosion on the rebars is the thickness of the concrete cover. Steel fibres are much less vulnerable to corrosion and will enhance the durability of the concrete. This makes it possible to design slimmer constructions.

At loading, the forces are transmitted to the fibre reinforcement in the same way as for reinforcement bars. The difference is that fibre reinforcement needs less strain to be activated in comparison to reinforcement bars. This leads to smaller crack widths in the concrete.

Use of fibres in concrete today

Fibres are commonly used in sprayed concrete for rock support. Concrete is sprayed directly on rock walls or inside tunnels. Set accelerating admixtures are added to the concrete, to make it set immediately in contact with the surface. Fibres give the sprayed concrete increased fracture toughness but the flexural tensile strength and the compressive strength are unchanged for this type of concrete[2]. Fibres are added in approximately 1 vol-%. The concrete becomes more ductile and is capable of resisting large deformations[9].

Fibre reinforced concrete is also used in other non-bearing structural parts such as slabs on ground, and pavement.

Future use of fibres in concrete

The goal is to use fibres in load-bearing structures as a replacement or together with reinforcement bars.

1.2 Fibre types

There are several different fibre types that can be used in concrete. The fibres vary in size, design and material. The most commonly used materials are steel, polymer, glass and carbon. All fibres used in concrete are to be tested and declared in relation to properties affecting the fibres suitability as reinforcing material[5]. The cross section of the fibres can be round, flat, crescent etc. An important factor for bonding between the fibre and the concrete matrix is the fibre shape. Common fibre shapes are end hooks, end knobs, twisted shape or wave shape.

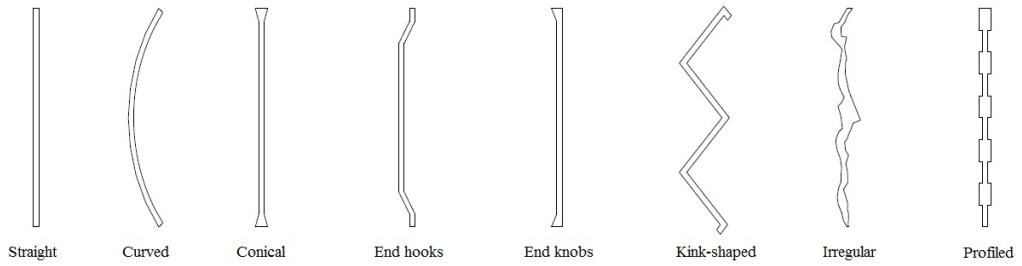

Figure 1: Different fibre shapes[5]

1.2.1 Steel fibres

Steel fibres are defined as straight or deformed pieces of steel suitable to be homogeneously mixed into concrete or mortar[13]. The fibres are classified into five groups as follows:

Group I : cold-drawn wire
Group II : cut sheet
Group III : melt extracted
Group IV : shaved cold drawn wire
Group V : milled from blocks

1.2.2 Polymer fibres

Polymer fibres can be made by different polymeric materials or a blend of them. The fibres shall be straight or deformed pieces of polymer witch are suitable to be homogeneously mixed into concrete or mortar[14]. Polymer fibres are classified in accordance with their physical form:

Class Ia Micro fibres: $<$ 0,30 mm in diameter; Mono-filamented
Class Ib Micro fibres: $<$ 0,30 mm in diameter; Fibrillated
Class II Macro fibres: $>$ 0,30 mm in diameter

1.3 Strength contribution from fibres

Fibres will generally increase the tensile strength of the concrete when cracking occurs, by transferring stress across the cracks. The ability to transfer stresses will remain relatively stable even as the crack widths increase. For design purposes, the tensile strength contribution from the fibres can be assumed to be distributed over the cracked concrete cross-section as a rectangular, ideal-plastic stress block.[5] This stress block is known as the residual tensile strength $f_{ftk,res2,5}$, and is an important parameter in design and classification of fibre reinforced concrete. The tensile strength is calculated from the flexural tensile strength $f_{Rk,i}$, which can be determined by testing of standard beams.

1.3.1 Determining the residual flexural tensile strength

The residual flexural tensile strength can be determined by the test method described in NS-EN 14651[12], The test method is based on a 3-point bending test of standard beams with dimensions 150x150x550 mm as shown in figure 2.

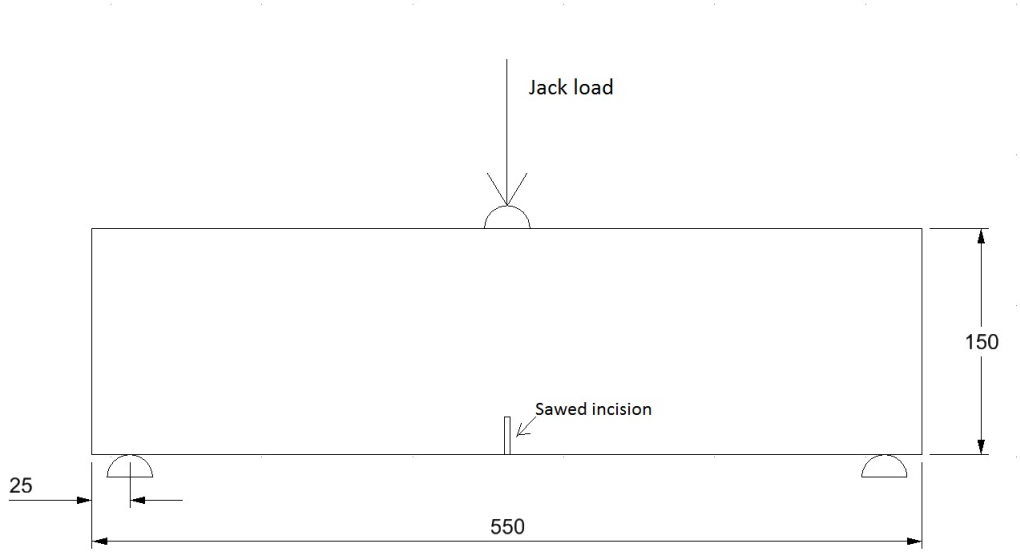

Figure 2: Test setup for measuring flexural tensile strength

The beams have a sawed notch at the middle to ensure that the main crack occurs at this point. Inductive sensors monitor the deflection Δ of the mid-point during testing, and a load-deflection diagram is computed. The crack width, also known as CMOD (Crack Mouth Opening Displacement) is related to the deflection, and the COIN-guidelines[5] derives the following relation between the deflection and CMOD:

$$\Delta = 0,85 \cdot CMOD + 0,04mm$$

From this equation, CMOD can be calculated for a given deflection, and a load-CMOD diagram can be established as in figure 3 .

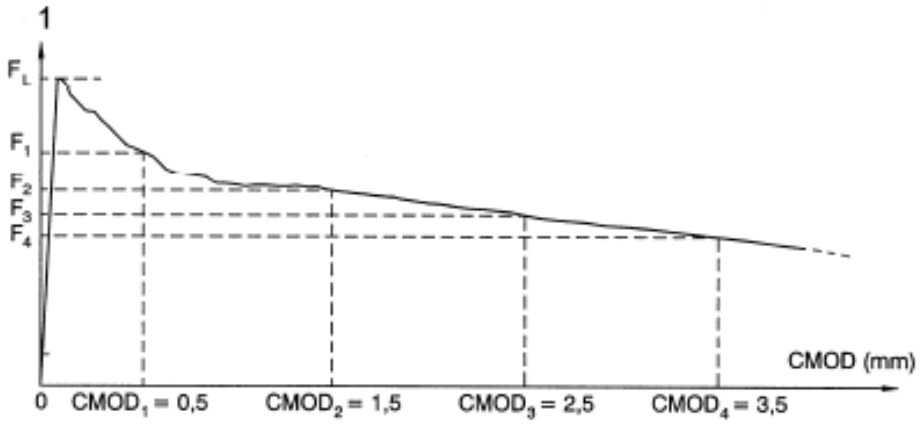

Figure 3: Load-CMOD diagram[12]

In classification and design, $f_{ftk,res2,5}$ is the tensile strength corresponding to the flexural tensile strength measured at CMOD 2,5 mm, denoted as $f_{Rk,3}$. However, the flexural tensile strength is calculated from the bending moment assuming linear stress distribution, which does not represent a realistic fibre effect. In order to find the correct tensile strength, the flexural tensile strength value must therefore be converted according to the relation between the two stress distributions in figure 4.

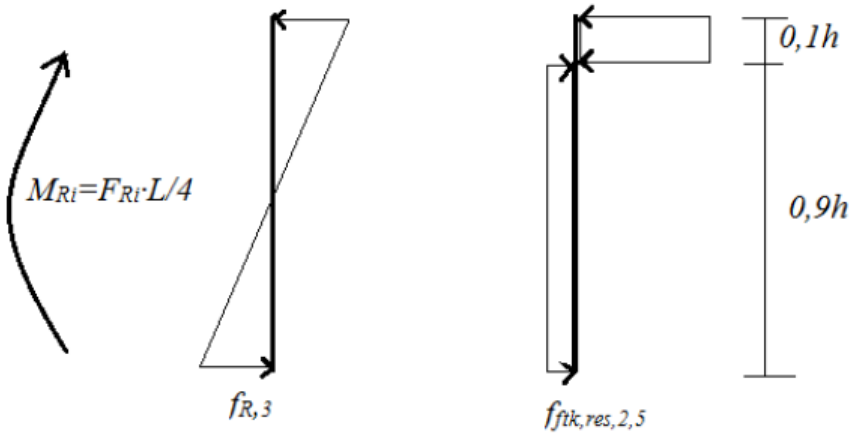

Figure 4: Relation between stress distribution for flexural tensile strength and tensile strength[5]

The COIN-report [5] has derived the following relation between $f_{ftk,res2,5}$ and $f_{Rk,3}$ based on the two stress distributions representing the same bending moment:

$f_{ftk,res2,5} = 0,37 \cdot f_{Rk,3}$

1.3.2 Classification

Fibre concrete is classified based on compression strength in the same way as conventional concrete. In addition, it is classified based on the residual tensile strength at CMOD 2,5 mm, $f_{ftk,res2,5}$.

Class	R0,5	R0,75	R1,0	R1,5	R2,0	R2,5	R3,0	R3,5
$f_{ftk,res2,5}$	0,5	0,75	1,0	1,5	2,0	2,5	3,0	4,0
$f_{Rk,3}$	1,3	2,0	2,7	4,0	5,4	6,7	8,1	10,8

Table 1: Classification based on residual tensile strength [5]

1.4 Standards and regulations

There is no uniform design guideline for fibre reinforced concrete. Several countries have made their own proposals for the use of fibre reinforced concrete.

COIN - Concrete Innovation Centre - is a centre for research based innovation in Norway. COIN has published a proposal guideline for design, execution and inspection of fibre reinforced concrete structures; COIN Project report 29-2011 [5]. The guideline refers mainly to NS-EN 1992-1-1 (EC2) for design rules, NS-EN 206-1 for production and NS-EN 13670 for execution. For testing of specimens and determination of resistance, EN 14651 is the most important basis.

The International Federation for Structural Concrete (*fib*), is preparing a new Model Code which contains new topics including fibre reinforced concrete. The last fib Model Code from 1993 can be considered as the basis for EC2[21].

2 Material properties

2.1 Ultra high performance fibre reinforced concrete

This section is based on COIN, State of the art report - Ultra High Performance Fibre Reinforced Concrete[4].

Ultra high performance fibre reinforced concrete (UHPFRC) is not a precise defined material, but it is commonly accepted to have a compressive strength above 150 MPa. Typical compressive strength is in the range of 150-220 MPa, but higher is also possible. Concrete with this high compressive strength is usually very brittle and will fail suddenly and dramatic when subjected to compressive loading. The addition of fibres make the concrete more ductile and failure will be less dramatic. The ductility properties added by the fibres depend on the fibre content, fibre geometry, fibre stiffness, fibre orientation and fibre length in relation to maximum aggregate size.

The concrete mix of a UHPFRC is characterized by a low w/b ratio, large amount of binder, low aggregate size and a large amount of super plasticizer (SP). The matrix of a UHPFRC need to be very dense. To get the matrix dense, it is important to obtain maximum packing density of all granular constituents. This is achieved by adding fine addition, such as silica fume. The w/b ratio is typically between 0,16 and 0,20, which means that not all of the cement will react with water. The remaining cement will contribute to the particle packing as an inert addition in the matrix. The amount of cement is about twice as high compared with normal concrete. The aggregate size is of importance regarding the packing density. Average aggregate size in UHPFRC is often below 1 mm, but coarser aggregate can be used. The mechanical strength of the aggregate has to be high to not become the weak part of the concrete, i.e. bauxite or granite. SP is crucial to obtain workability in UHPFRC due to the low w/b ratio. A typical dosage of SP in UHPFRC is up to 5 mass-% of the cement. The fibres in UHPFRC give the "performance". It enhances the ductility in tension and compression and it increases the tensile and flexural strength. Best results are obtained with approximately 2,5 vol% fibres with l/d between 40 and 60.

2.2 Fibre reinforced lightweight aggregate concrete

This section is based on the COIN report "Lightweight aggregate concrete - Improvement of ductility by using fibre reinforcement"[3].

Lightweight aggregate concrete (LWAC) is as the name implies, a concrete produced with low density aggregates. To be denoted LWAC, the concrete density have to be lower than 2000 kg/m^3. If the density is below 1000 kg/m^3, the concrete can be

defined as a super lightweight aggregate concrete (SLWAC). Properties and technical requirements for lightweight aggregates are specified in EN 13055-1. The use of LWAC is limited due to its lack of ductility. The lightweight aggregate used to produced LWAC is usually weaker than the cement matrix, and provides lower resistance to crack development compared to normal concrete. This makes LWAC a very brittle material.

When adding fibre reinforcement to LWAC, the fracture toughness can be improved significantly. The improvement depends on the fibre type, fibre amount and the bonding between fibres and concrete. Experimental testing on macro fibres in LWAC show promising behaviour concerning the ductility after cracking. When adding fibre to lightweight concrete, the risk of fibre separation has to be considered, especially when using steel fibres. Steel fibres have a high density, and will sink in a concrete mix with lightweight aggregate. This can be avoided with a well graded concrete and a viscous matrix phase.

2.3 Self-compacting fibre reinforced concrete

2.3.1 Flowability of fresh concrete

The properties of fresh concrete is important for a successful casting process. The target is to ensure workability without risking segregation. One of the main intentions with fibre reinforced concrete, is to reduce the necessary work with reinforcement binding and vibration. A good approach to achieve this, is to use self compacting concrete. The flowability aspect is especially important for self compacting concrete, since the purpose of SCC is to fill the form by self-weight alone without any vibration. It may be difficult to design a concrete mix that is flowable enough to fill the form by itself without any blocking, and at the same time be viscous enough to avoid segregation. Adding fibres to the SCC makes it even more difficult to control the rheological properties of the fresh concrete. Steel fibres can severely reduce flow, and too much fibres may lead to lumping of fibres during the casting.

A theoretical approach to the fresh concrete properties, is to assume that the concrete behaves as a Bingham plastic fluid. This means that the concrete will not start to flow until it reaches its critical yield shear stress τ_0. After reaching this yield stress, there is a linear relation between the shear rate γ and the resulting shear stress τ in the concrete. The slope of the line is called the plastic viscosity μ. The following relation is valid for bingham fluids:

$\tau = \tau_0 + \mu \cdot \gamma$ [18]

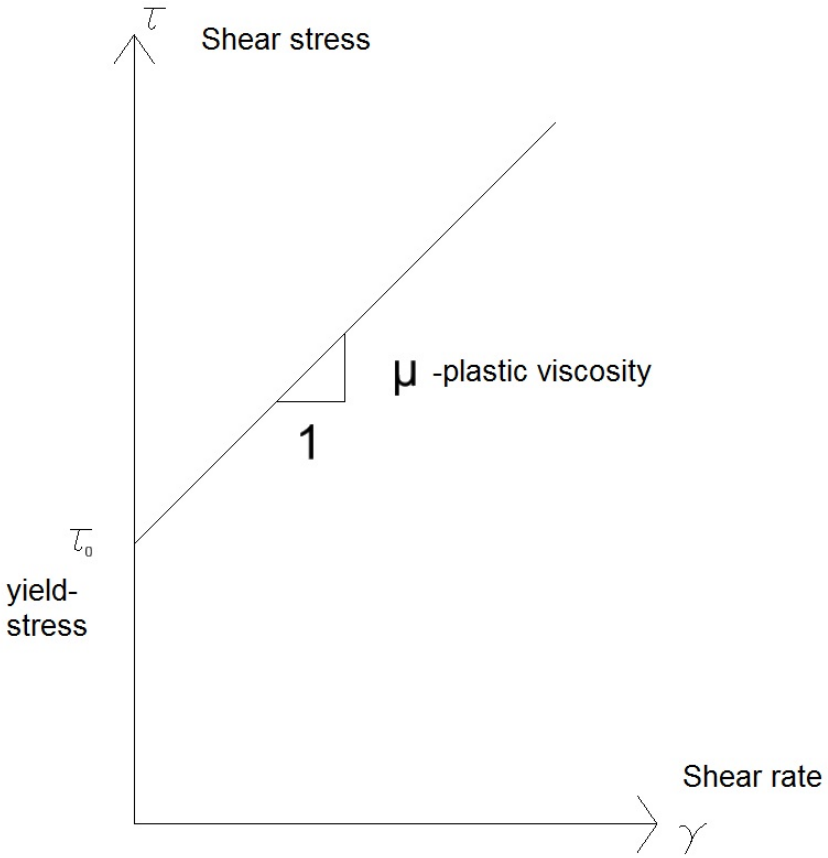

Figure 5: Bingham-model behaviour

For the fresh self compacting concrete this means that the shear stress from the self-weight must exceed the yield stress in order for the flow to start. As a result, self compacting concrete has a very low yield value τ_0 compared to standard-flow concrete, while the plastic viscosity μ is approximately the same.[1]

Superplasticizer is commonly used to enhance the workability of fresh concrete. Superplasticizer will reduce the yield stress τ_0, but studies suggest that it will have a relatively minor effect on the plastic viscosity μ.[20]

The yield shear stress and the plastic viscosity are two important parameters for understanding the rheology of the fresh concrete and several test methods are developed in order to estimate these parameters. The two-point test [18] may be used, but also test methods that use the correlation between yield stress and slump flow have been developed, e.g. the 4C-Rheometer and the LCPC-box. The relation between yield stress and plastic viscosity can be used to assess the risk of segregation, and reveal challenges that may occur during casting. Figure 6 is from the manufacturer of the 4C-Rheometer, and shows the fresh concrete properties related to the yield stress and plastic viscosity.

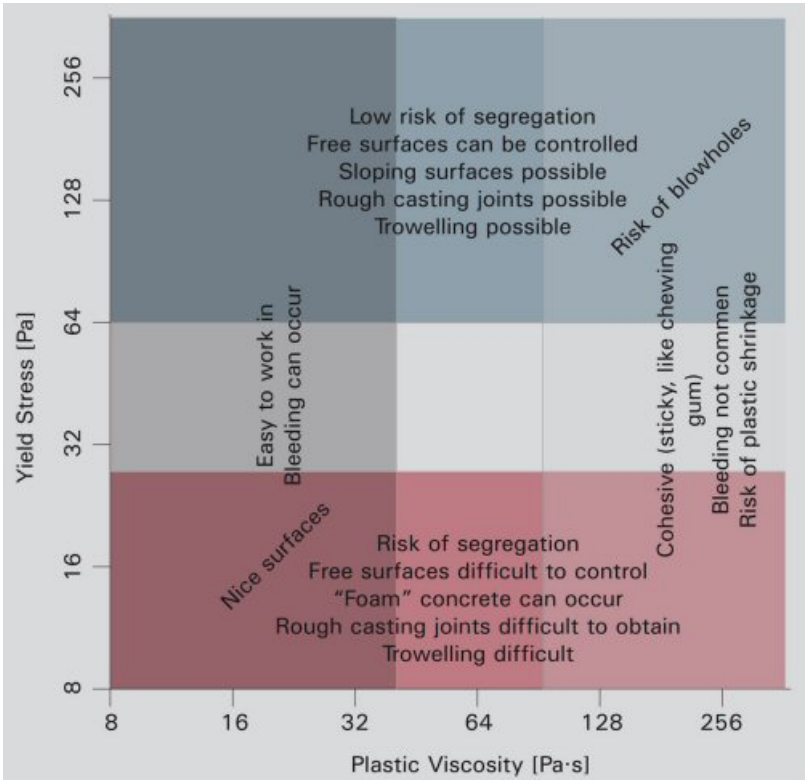

Figure 6: Fresh concrete properties related to τ_0 and μ[20]

Slump flow test

The slump flow test is a simple test used instead of the slump measure for self compacting concrete. The test is performed when the concrete arrives at the casting site to check if the concrete has the desirable flow before casting starts. A cone is placed on a plate and filled with concrete. After the cone is lifted, these observations are made:

- final flow diameter
- the time it takes for the flow to reach a diameter of 500mm (t500)
- state of the concrete edge, to check for separation/bleeding

4C-Rheometer

This test is based on the slump flow test, but the cone is lifted by a machine connected to a computer. In addition, a camera is monitoring the flow speed and spread diameter. The rheometer uses the video to determine the spread versus time, and a program is able to calculate both the plastic viscosity and the yield stress. The yield stress is determined based on a relation where the yield stress is a function of slump-flow and density, while the plastic viscosity is estimated using a detailed extraction of the flow curve[20]

LCPC-BOX

This test is developed at LCPC (Laboratoire Central des Ponts et Chaussées). The LCPC-box is a rectangular shaped box with plane edges. Six liters of concrete is poured at one end of the box and will start to flow. After the flow stops, the spread length L, and the height at starting point h_0 is measured. These two parameters can be used to determine the yield stress, either by the formulas or the diagram presented by N. Roussel [16]. Visual observations during the test also give a good indication on how well the fibres are transported with the concrete flow.

(a) side-view of concrete flow[16]

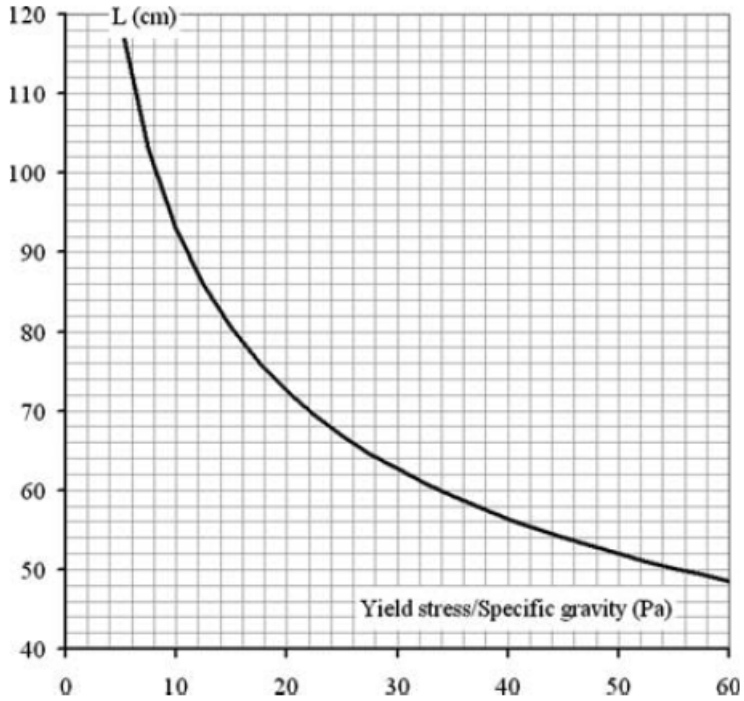

(b) Relation between spread length and yield stress[16]

Figure 7: LCPC-BOX

3 Moment Capacity

The main topic for this master thesis is to study fibre reinforced load carrying structural parts, with focus on moment capacity of beams. Steel fibres contribute to the moment capacity of a concrete section by giving the concrete a residual tensile strength after cracking, $f_{ftk,res2,5}$, as described in 1.3. This contribution must be taken into account when determining the moment capacity of a fibre reinforced cross-section.

3.1 Simplified method

Coin Project Report 29-2011 gives a simplified method of calculating moment capacity for fibre reinforced concrete. The method can be used for both fibre concrete and reinforced fibre concrete. This method incorporates the residual tensile strength provided by the fibres. In design, the characteristic value is divided by a safety factor as in common practice. $f_{ftd,res2,5} = f_{ftk,res2,5}/\gamma_{cf}$.

3.1.1 Fibre concrete

Capacity of a cross section only reinforced by fibres can according to the COIN-guidelines be calculated simplified by assuming that $f_{ftd,res2,5}$ acts on 0.8h and the inner moment arm is 0.5h as shown in figure 8. The moment capacity can then be derived as:

$$M_{Rd} = 0.4 \cdot f_{ftd,res2,5} \cdot b \cdot h^2$$

Where

b =Cross section width

h =Cross section height

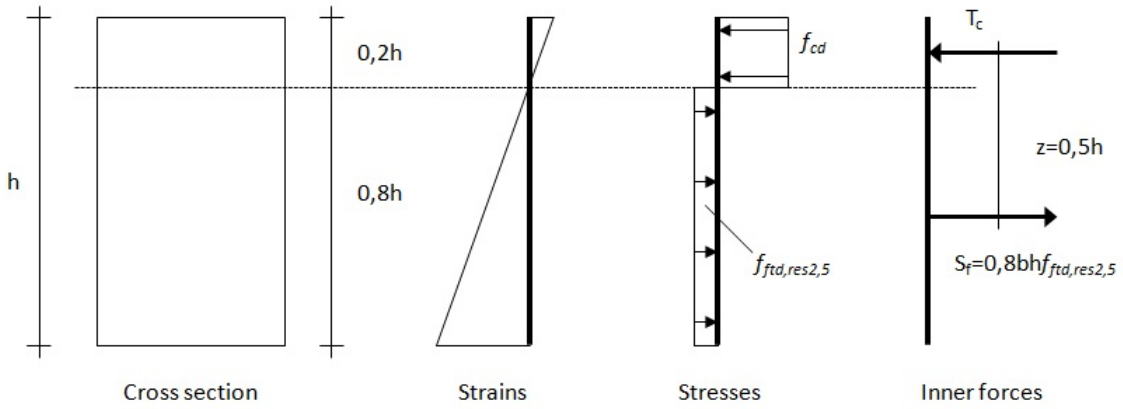

Figure 8: Strain and stress distribution for a rectangular fibre reinforced cross-section[5]

This simplified calculation applies for fibre concrete with $f_{ftd,res2,5}$ lower than 2.5MPa. If it is higher, the compression zone has to be defined by demanding axial equilibrium of the inner forces in the cross section.

3.1.2 Reinforced fibre concrete

Moment capacity of reinforced concrete with fibres is based on load carrying interaction between the reinforcement bars and the fibres. The work-diagram for the conventional reinforcement is as described in EC 2 [3.2.7]. The concrete compression zone is characterized as in EC 2 [3.1.7]. The tension capacity of the fibre reinforced concrete is included as a constant stress along the tension zone height.

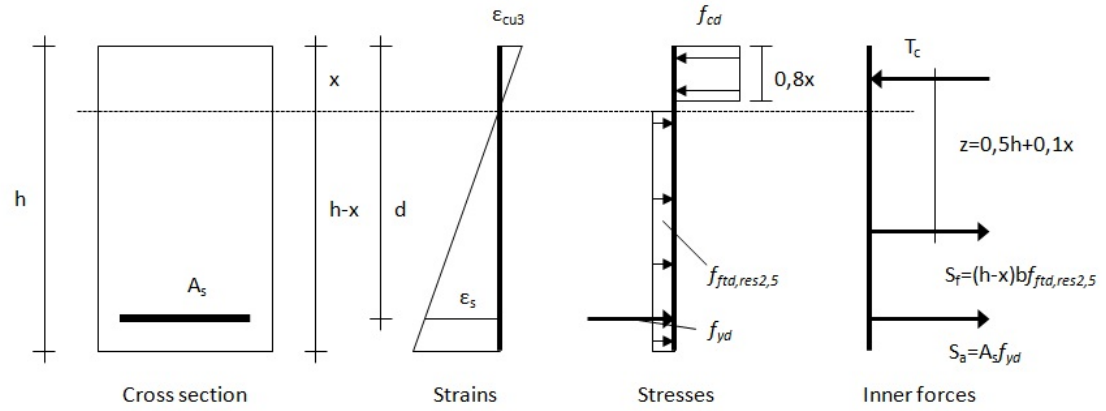

Figure 9: Strain and stress distribution for a rectangular cross-section of reinforced fibre concrete[5]

Axial equilibrium gives the following relationship:

$T_c = S_a + S_a$

where

$T_c = 0.8 \cdot x \cdot b \cdot f_{cd}$

$S_f = (h - x) \cdot b \cdot f_{ftd,res2,5}$

$S_a = A_s \cdot f_{yd}$

And

x =Compression zone height

f_{cd} =Design concrete compressive stress

f_{yd} =Design reinforcement stress

A_s =Reinforcement area

d =Effective cross sectional height

The compression zone height x, can be determined by extracting it from the equations granted axial equilibrium. The formula can be written as:

$x = \frac{A_s \cdot f_{yd} + h \cdot b \cdot f_{ftd,res2,5}}{0.8 \cdot b \cdot f_{cd} + b \cdot f_{ftd,res2,5}}$

The moment capacity can then be determined by moment equilibrium about the compression resultants point of attack:

$M_{Rd} = S_f \cdot (0.5h + 0.1x) + S_a \cdot (d - 0.4x).$

3.2 Multi-layer method

The Multi-Layer Method is a good tool for calculating moment capacity, and to reproduce experimental results from bending tests. The calculations are easiest done on a computer, for instance by using a spreadsheet in Excel. This method works well for several types of rectangular concrete cross sections, both conventionally reinforced and fibre reinforced.

The method is based on axial equilibrium within the cross section, and linear strain distribution along the height. The cross section is divided into a predefined number of layers across the height. This makes it possible to calculate the average stress in each layer and in the reinforcement with a given strain as input.

When this model is used with fibre reinforced concrete, the tension zone in the cross section will have a stress contribution from the fibres. For calculations we can use the capacity $f_{ftk,res2,5}$ as a rectangular stress block in the tension zone. COIN Project report 29-2011 recommends an upper limit for tension strain in the tension edge to be $\frac{3}{h}‰$. Properties of concrete in compression and rebars can be found in EC 2.

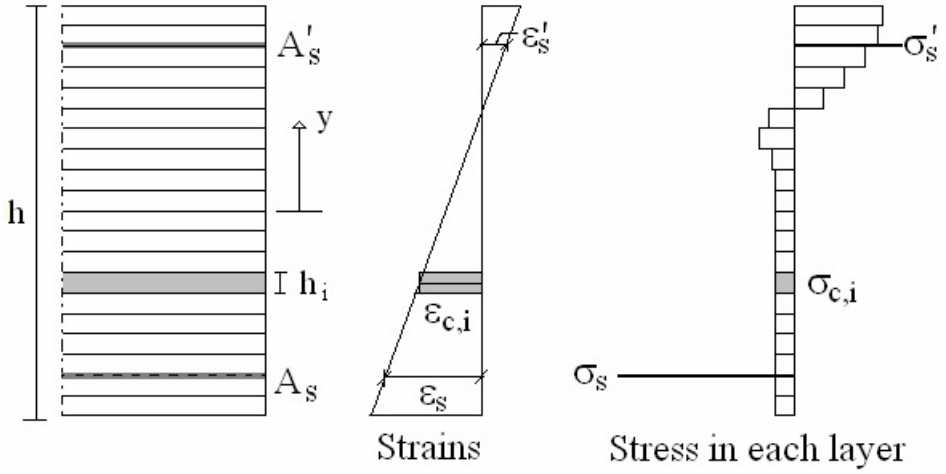

Figure 10: Multi-layer method: stress and strain distribution in sections[17]

Calculation of moment capacity is performed by demanding axial equilibrium of the

forces in the cross section. This leads to the moment capacity at any given state of strain.

$N = \sum \sigma_{c,i} \cdot t \cdot \frac{h}{n} = 0$

$M = \sum \sigma_{c,i} \cdot t \cdot \frac{h}{n} \cdot y_i$

If there are rebars in addition to the fibre reinforcement, the formulas need to take account for that.

$N = \sum(\sigma_{c,i} \cdot t \cdot \frac{h}{n}) + \sigma_s \cdot A_s = 0$

$M = \sum(\sigma_{c,i} \cdot t \cdot \frac{h}{n} \cdot y_i) + \sigma_s \cdot A_s \cdot y_i$

Where:

$\sigma_{c,i}$ =Concrete stress in layer i

t =Layer thickness

n =Number of layers

σ_s =Reinforcement stress

y_i =Distance from the centre line of layer i to the the cross sectional centre of gravity

y_s =Distance from the reinforcement centre of gravity to the cross sectional centre of gravity

3.3 Shear control

The COIN Project report[5] gives a suggestion for calculating the shear capacity of fibre reinforced concrete. The rules only apply for steel fibres. The contribution to shear capacity from steel fibres is well documented by experimental studies, but it is not documented that synthetic fibres have the same contribution. The rules apply for structural parts where the relationship between span and cross section height is larger than 3 ($\frac{l}{h} > 3$), for two sided support and ($\frac{l}{h} > 1,5$) for cantilevered parts.

There are several methods and models available for calculation of shear capacity in fibre reinforced concrete. The method taken from the COIN guidelines are based on beam test series with conventional bar reinforcement in the tension zone of the beam. Thus, the rules only apply for cross sections with bar reinforcement and fibre reinforcement.

Shear capacity is calculated as in EC 2, shear capacity of concrete without stirrups, with the fibre contribution as an addition.

$V_{Rd,c} = V_{Rd,ct} + V_{Rd,cf}$

$V_{Rd,ct}$ is the contribution from the concrete and the bar reinforcement. $V_{Rd,cf}$ is the contribution from the fibre reinforcement.

$$V_{Rd,ct} = [C_{Rd,c} \cdot k \cdot (100\rho_l \cdot f_{ck})^{1/3} + k_1 \cdot \sigma_{cp}] \cdot b_w \cdot d \geq (v_{min} + k_1 \cdot \sigma_{cp}) \cdot b_w \cdot d$$

$$V_{Rd,cf} = 0,6 \cdot f_{ftd,res2,5} \cdot b_w \cdot h$$

Where:

$C_{Rd,c} = \frac{k_2}{\gamma_c}$

$k_2 = 0,15$ or $0,18$ depending on the aggregates in the concrete mix

$k_1 = 0,15$ in compression and $0,3$ in tension

$\rho_l = \frac{A_s}{b_w \cdot d} \leq 0,02$

b_w =Width of cross section web

$\sigma_{cp} = \frac{N_{Ed}}{A_c} \leq 0,2 \cdot f_{cd}$ where N_{Ed} =Axial force from external loading or pre-stressing

$k = 1 + \sqrt{200/d} \leq 2$

$v_{min} = 0,035 \cdot k^{2/3} \cdot f_{ck}^{1/2}$

4 Serviceability Limit State

4.1 Cracks

Cracks in concrete can occur due to loading, volume changes or chemical attacks. In this thesis, cracks due to loading is emphasized since this is most relevant for the beams to be tested.

Cracks will occur when the concretes tensile strength is exceeded, and the tensile forces need to be transferred to the reinforcement. Since the reinforcement needs to transfer all the stress across the cracks alone, the strain in the reinforcement is large in the cracked cross-sections, and smaller in the uncracked sections where the concrete is still active. The case is opposite for the concrete, which will have no strain in the cracks, and larger strains between the cracks. This strain variation is illustrated in figure 11 from Sørensen[19]. In order to estimate the crack widths, mean values of the strains in both reinforcement and concrete are used as parameters, denoted ε_{sm} and ε_{cm} respectively.

Fibres will to a great extent contribute to reducing cracks because of its ability to transfer stress across the cracks. The tensile strength contribution from the fibres $f_{ftk,res2,5}$, will result in a decreased stress in additional reinforcement bars, and increased compressive zone αd.

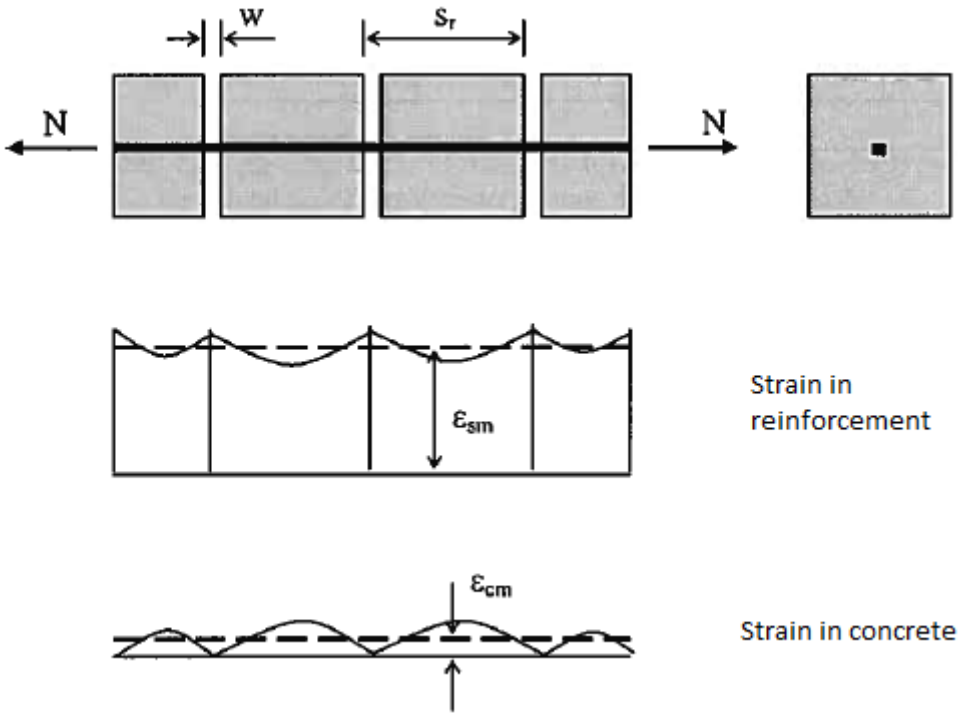

Figure 11: Strains in cracked beam[19]

EC2 chapter [7.3.4] gives guidelines for estimating the crack widths for conventionally reinforced concrete. The COIN guidelines are based on the method described in EC2, but some of the parameters are modified in order to take account for the fibre effect. The formula for calculating the crack width is based on the mean strain values and the fact that the deformation in the concrete must be equal to the deformation in the reinforcement:

$$w_k = s_{r,max} \cdot (\varepsilon_{sm} - \varepsilon_{cm})$$

were

w_k- crack width

$s_{r,max}$−maximum crack distance

ε_{cm}−mean strain in concrete

ε_{sm}- mean strain in reinforcement

Further, EC2 gives an expression for the strain difference $(\varepsilon_{sm} - \varepsilon_{cm})$ as:

$$(\varepsilon_{sm} - \varepsilon_{cm}) = \frac{\sigma_s - k_t \cdot \frac{f_{ct,eff}}{\rho_{p,eff}} \cdot (1 + \alpha_e \cdot \rho_{p,eff})}{E_s} \geq 0,6 \cdot \frac{\sigma_s}{E_s}$$

σ_s−Stress in reinforcement for a cracked cross-section

$\alpha_e = \frac{E_s}{E_{cm}}$

$\rho_{p,eff} = \frac{A_s}{A_{c,eff}}$, $A_{c,eff}$- Effective area of the concrete tensile zone

$k_t = 0,6$ for short term loading, and 0,4 for long term loading

To find the strain difference, the stress in the reinforcement σ_s is needed. This can usually be found by using the following expression[19]:

$$\sigma_s = E_s \cdot \frac{M(1-\alpha) \cdot d}{EI}$$

However, the fibre effect must be taken into consideration when calculating σ_s. The fibres will decrease the tension in the reinforcement bars, but it is difficult to assume an exact stiffness for a fibre reinforced section. The most practical solution to this problem, is to extract the value of σ_s directly from multi-layer method calculations for a given moment. In this thesis, σ_s was found in this way, using the multi-layer program in excel.

The last parameter that is needed to determine the crack width is the maximum crack distance, $s_{r,max}$. This parameter is found as described in EC2, but an extra factor k_5 is added to the formula to adjust for the fibre effect.

$$s_{r,max} = k_3 \cdot c + k_1 \cdot k_2 \cdot k_4 \cdot k_5 \cdot \frac{\phi}{\rho_{p,eff}}$$

k_1−0,8 for rebars with good bonding, 1,6 for rebars with smooth surface

k_2−0,5 for bending, 1,0 for pure tensile force

k_3−3,4

k_4−0,425

k_5−(1-$f_{ftk,res2,5}/f_{ctm}$)

ϕ- bar diameter

Another parameter of interest is the mean crack distance $s_{r,m}$. The COIN report suggests using the same expression as recommended in EC2 $s_{r,m} = \frac{s_{r,max}}{1,7}$.

4.2 Minimum reinforcement

4.2.1 Background

In design of concrete structures in serviceability limit state (SLS), there is a demand for minimum reinforcement to control cracking. Cracking can occur as a result of thermal expansion, shrinkage or loading. The minimum area of reinforcement ensures ductile behaviour and ensures that the capacity of the tensile zone is not reduced after cracking starts. In conventionally reinforced concrete, the tensile forces are transferred to reinforcement bars through bonding, and when the concrete tensile strength is exceeded, there is a sudden transfer of stress to the reinforcement. If the requirements for minimum reinforcement are met, the rebars will not yield when cracking starts. This leads to a more favourable distribution of cracks and smaller crack widths, instead of a few wide cracks.[6]

In fiber reinforced structures, the fibres will transfer stress across the cracks. This will increase the tensile strength and contribute to limit cracking. As a result, the demand for longitudinal bars is reduced.

4.2.2 Design guidelines

EC2 describes minimum reinforcement in chapter 7.3.2. The formula for necessary reinforcement is derived from equilibrium between the tensile force in the concrete before cracking, and the tensile force in the reinforcement at yielding.

$$A_{smin} \cdot \sigma_s = k_c \cdot k \cdot f_{ct,eff} \cdot A_{ct}$$

A_{smin}= Minimum area of reinforcement

σ_s= stress in reinforcement, normally set to the yield stress f_{yk}

k_c= stress distribution coefficient

k = non-linear stress distribution coefficient - leading to a reduction in restraint force

$f_{ct,eff}$= tensile strength of concrete at time of cracking, set to f_{ctm} after 28 days

A_{ct}= area of concrete within the tensile zone

This formula is applied for traditionally reinforced structures. For fiber reinforced concrete the formula can be modified into taking account for the effect of the fibres. COIN-report 29 [5] suggests a formula where the fibre effect is included:

$$A_s \cdot \sigma_s + A_{c2} \cdot f_{ftk,res2,5} \geq A_{ct} \cdot f_{ct,eff}$$

or

$$A_{smin} \geq (A_{ct} \cdot f_{ftk,res2,5})/\sigma_s$$

The fibre contribution is expressed as the concrete area after cracking, A_{c2}, multiplied with the residual tensile strength $f_{ftk,res2,5}$. If the requirements for minimum reinforcement are met, the structure will automatically achieve hardening behaviour on the load-deformation diagram. This means that the loading can be increased further after cracking has started, which is a necessary condition to apply the guidelines in the COIN-report.

Beams

It has been performed comprehensive testing with fibres in beams and the contribution from the fibres is well documented. For rectangular beams, the required minimum reinforcement can be determined as: [5]

$$A_{s,min} = 0,26 \cdot b_t \cdot d \cdot (f_{ctm} - 2,1 \cdot f_{ftk,res2,5})/f_{yk}$$

But

$$A_{s.min} \geq 0,0013 \cdot b_t \cdot d \cdot (1 - 2.1 \cdot f_{ftk,res2,5}/f_{ctm})$$

Part II

Experimental design

5 Design of beams

5.1 Beam types

The experimental part of the thesis included casting and testing of six full scale beams, six standard beams and six standard cubes. Dimensions and volumes are tabulated in table 2 below.

Type	Number of specimens	Dimensions [mm]	Volume [L]	Total volume [L]
Full scale beams	6	200x300x4000	240	1440
Standard beams	6	150x150x550	12,375	74,25
Standard Cubes	6	100x100x100	1	6

Table 2: Overview of casting elements

The full scale beams were to be reinforced with different amounts of conventional reinforcement bars, in addition to the 1% dramix 65/60 fibre content in the concrete mix. The beams were divided into three types, with two equally reinforced beams of each type for comparison. The different beam types should be reinforced in order to provide a good basis for estimating the fibre strength contribution, as well as the effect of reinforcement bars combined with fibres. With regard to this, the first beam type was decided to only be fibre reinforced, while the two other types would have longitudinal reinforcement bars combined with the fibres. The contribution from the reinforcement bars is of interest with respect to both strength and crack distribution. However, it was important that the amount of reinforcement bars was not too high, risking shear failure in the beams. The cross-section of the beams should stay under-reinforced to avoid failure in the compression zone. As a preliminary estimate, the following beam types were suggested as basis for design calculations:

Beam Type	Fibre Content	Reinforcement Bars
M3	1%	None
M2	1%	~ minimum area of reinforcement
M1	1%	more, but still under-reinforced

Table 3: Design conditions for large beams

5.2 Test setup

5.2.1 Full scale beam test

The full scale beams were to be tested in bending to get moment failure. To conduct the testing, a 1000 kN jack was put to disposal in the laboratory. To get a moment failure, two different test methods are typically used; a three point bending test or a four point bending test. The difference between these two tests is that the three point test only gives maximum moment directly under a point load, but the four point test will distribute the maximum moment along the beam length between two load points. With a larger area of maximum moment, the beam will more likely fail where the concrete is weakest. This is more like a real situation where cracks and failures typically occur where the concrete is weak. Also, comparing crack widths within the area between the point load is relevant, since the cross-section is exposed to the same bending moment along this length.

The beams were chosen to be tested in a four point bending test. To get a four point bending situation, a steel beam with two support points at the ends is placed on top of the test beam. This steel beam then gets pushed by the jack and distributes the point load into two equal point loads on top of the test beam. The principle of the test setup is shown in figure 12.

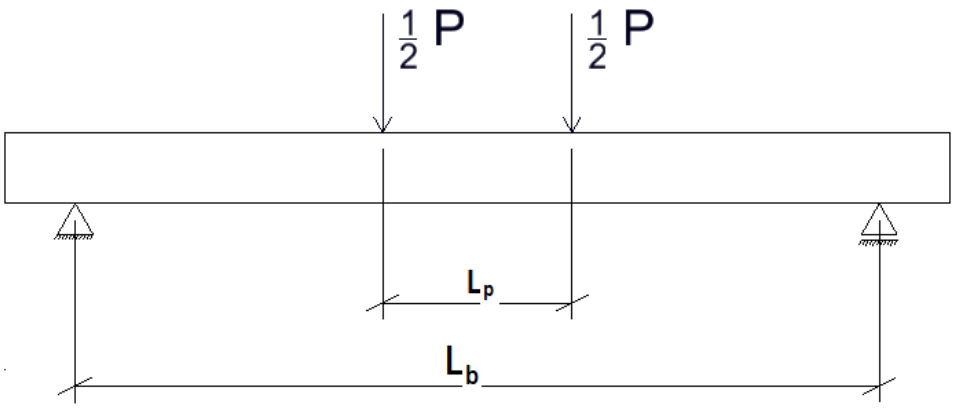

Figure 12: 4-point bending test

The beam span and the load placement influence the behaviour and the failure mechanism in the beam, so a suitable setup has to be chosen. Two factors are of concern; the beam span L_b and the distance between the two point loads L_p. The shear force in the beam has the same magnitude regardless of these factors, but the moment varies. To get an optimal test setup, the shear capacity has to be checked and different situations have to be calculated for moment capacity. A long beam span is desirable to get moment failure, but some length has to be outside the supports to ensure anchoring in beams with reinforcement bars.

5.3 Calculations

This chapter will go through all the calculations performed before testing of the full scale beams. Formulas and calculation methods used are as described in previous chapters.

Beam data

The six beams were designed with a B35 ($f_{ck} = 35MPa$) concrete and 1 vol-% steel fibres. The residual tensile strength $f_{ftk,res2,5}$ could not be determined before the concrete had been tested, but the value was set to $2,0MPa$ as advised by Terje Kanstad. All material and safety factors in the calculations were put to $1,0$ to estimate the correct failure loads. The beam span and the load span used in the beam testing had to be decided before the jack load at failure could be calculated. Dimensions were decided to be:

Beam span $L_b = 3400mm$

Load span $L_p = 800mm$

Final test setup with dimensions is shown in the figure below:

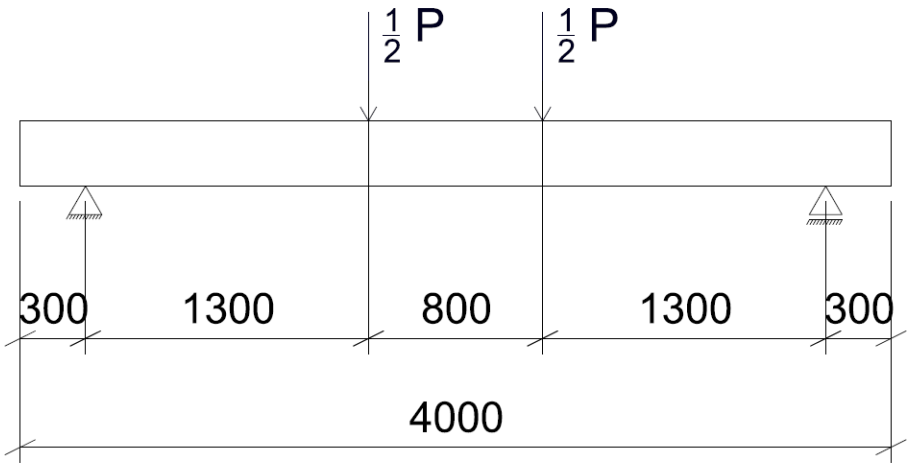

Figure 13: Test setup with location of loads and supports

5.3.1 Minimum reinforcement

Beam series M2 was to be designed with minimum required bar reinforcement. The formulas described in section 4.2.2 were used to calculate the minimum reinforcement for the beams. All of the beams had the same cross section and the same material composition, thus the calculated value for minimum reinforcement is valid for all

the beams. To calculate the minimum reinforcement values, the effective height of the cross section (d) had to be assumed. This value depends on the concrete cover and the diameter of the bar reinforcement. The thickness of the concrete cover was chosen to be $c = 25mm$, and reinforcement bars with diameter $12mm$ were used to assume the effective height. This gave an effective cross section height $d = 269mm$ used in the calculations.

Calculation with fibre contribution:

$$\begin{aligned} A_{s,min} = &\quad -27,976mm^2 \\ A_{s,min} \geq &\quad -21,856mm^2 \end{aligned}$$

The result shows that bar reinforcement is not necessary to satisfy the requirement for minimum reinforcement.

To get a reinforcement area value, the formulas for minimum reinforcement in EC2[11] are used.

$$A_{s,min} = 0,26 \cdot \frac{f_{ctm}}{f_{yk}} \cdot b_t \cdot d \geq 0,0013 \cdot b_t \cdot d$$

b_t is the average width of the tension zone. For the beams considered in this thesis, b_t is equal to the cross section width.

Calculated value for minimum reinforcement is then:

$$A_{s,min} = 89,5mm^2$$

The calculations are shown in appendix 1. One bar with diameter $12mm$ gives $A_s = 113,1mm^2$. This was chosen as the bar reinforcement in beam series M2. Beam series M1 was planned to have more bar reinforcement than M2, and after consultation with Terje Kanstad the reinforcement area was chosen to be three times as large in M1 as in M2. All the beams are tabulated below:

Beam series	no. of beams	bar reinforcement	A_s $[mm^2]$	fibre reinforcement
M1	2	3Ø12	339,3	1 vol-%
M2	2	1Ø12	113,1	1 vol-%
M3	2	none	0	1 vol-%

Table 4: Reinforcement design of large beams

5.3.2 Simplified method for moment capacity calculations

The simplified method shown in section 3.1 was used to calculate the moment capacity of the full scale beams. The shear capacity of the beams was also calculated to make sure the beams had higher shear resistance than bending resistance. Shear

capacity was calculated as described in chapter 3.3, shear control. Beam series M3 has no bar reinforcement, thus the capacity is calculated with the method showed in 3.1.1, fibre concrete. Beam series M1 and M2 have bar reinforcement in addition to fibre reinforcement. The moment capacities for M1 and M2 were calculated with the method presented in 3.1.2, fibre reinforced concrete. The calculations are shown in appendix 1. Table 5 shows the results of the calculations done on the different beams. The failure jack load (P_{Rd}) was calculated based on the test setup dimensions.

$P_{Rd} = \frac{M_{Rd}}{0{,}65m}$ Jack failure load for moment capacity

$P_{Rdv} = V_{Rdc} \cdot 2$ Jack failure load for shear capacity

Beam series	moment cap. M_{Rd} [kNm]	Shear cap. V_{Rdc} [kN]	max load bending P_{Rd} [kN]	max load shear P_{Rdv} [kN]
M1	55,96	113,75	86,09	227,49
M2	30,46	101,23	46,87	202,46
M3	14,4	72	22,15	144

Table 5: Capacity based on simplified method

The value for shear failure load in beam series M3 is only calculated as the fibre contribution to shear resistance, which is the same for all the beams, $P_{Rdv,cf} = 2 \cdot (0,6 \cdot f_{ftd,res2,5} \cdot b \cdot h)$. Based on the calculations, the shear resistance is in a magnitude of 2,6 to 6,5 times larger than the bending resistance. As a result, the beams will fail in bending as planned.

5.3.3 Multi layer method

The multi-layer method shown in chapter 3.2 has been used to estimate the moment capacity of the full scale beams. To perform the calculations, an excel spreadsheet with a built-in Solver function was used. The program is the same as the one used in the master thesis by Nordhus, Simpson, Steinnes[10]. The file can be found on the appendix CD.

The cross section was divided into 20 layers, with a layer height $h_i = 15mm$. The input values needed to run the program in the spreadsheet was cross section data and material data. The program calculates the strain distribution over the cross section height by assuming a linear strain distribution. To calculate the resulting stress in each layer, proper material models have to be chosen. By demanding axial equilibrium the moment capacity can be calculated for any given state of strain.

Material models

Material models for concrete in compression were taken from EC2 [11] section 3.1.7. For a concrete with $f_{ck} \leq 50MPa$, the strain at maximum stress is $\varepsilon_{c2} = 2‰$ and the strain in ultimate limit state is $\varepsilon_{cu2} = 3,5‰$ according to table 3.1 in EC2. In order to calculate the concrete stress when the strains are known, the model from EC2 is used. The upper strain limit for concrete in compression was put to $\varepsilon_{cu2} = 3,5‰$.

Strain	Stress
$0 \leq \varepsilon_c \leq \varepsilon_{c2}$	$\sigma_c = f_{cd} \cdot [1 - (1 - \frac{\varepsilon_c}{\varepsilon_{c2}})^n]$
$\varepsilon_{c2} \leq \varepsilon_c \leq \varepsilon_{cu2}$	$\sigma_c = f_{cd}$

where $n = 2,0$ for $f_{ck} \leq 50MPa$

For concrete in tension, a material model made by Åse Døssland [17] was used. The method incorporates the concrete tensile strength before cracking and the residual tensile strength after cracking. If the concrete tensile strength is higher than the residual tensile strength, the concrete will crack at higher stresses than the residual tensile strength.

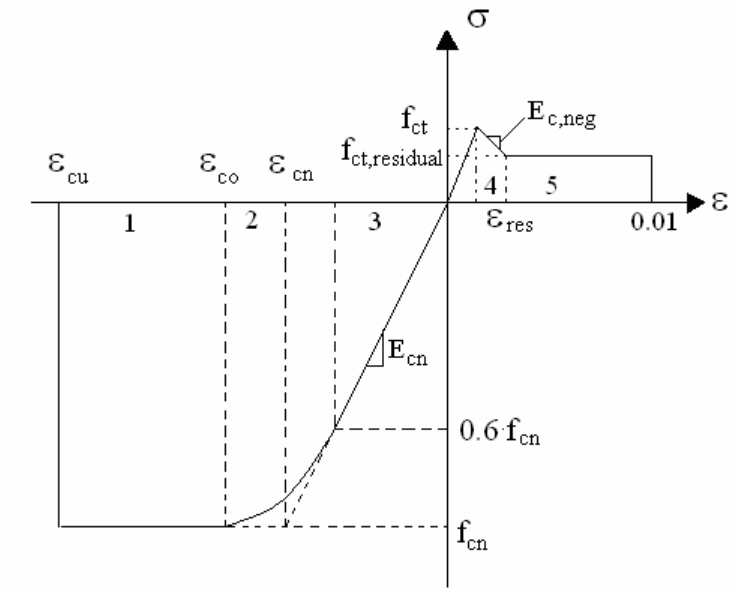

Figure 14: Stress-strain diagram for concrete including tension [17]

The values in figure 14 have been modified to EC2. The maximum strain value for concrete in tension was put to $\varepsilon_{uk} = 10‰$, the negative slope value used was $E_{c,neg} = 10000MPa$ and the concrete tensile strength for a B35 concrete is $f_{ctm} = 3,2MPa$.

Material model for reinforcement bars was taken from EC2 section 3.2.7. The yield strength of the reinforcement bars was put to $f_{yk} = 500MPa$. The hardening factor was found in EC2 table NA.3.5(901) and put to $k = 1,04$.

Beam series	Multi-layer moment capacity M_{Rd} [kNm]	Failure load P_{Rd} [kN]
M1	56,94	87,60
M2	30,92	47,57
M3	16,62	25,57

Table 6: Capacity based on multi-layer method

When all of the input data were entered into the program, a simulation for each beam type could be conducted. The results from the simulations are shown in the table below.

5.3.4 Control of anchoring capacity

When deciding the test setup distances, a free length outside the supports has to be considered for anchoring of the reinforcement bars. The necessary length depends on the stress in the reinforcement bars, which is related to the maximum shear force at supports. Since there are no stirrups in the beams, the crack angle may be assumed to be $\theta = 45^{\circ}$ and consequently the force in the bars ΔF_{td} is equal to the shear force V_{Ed} as described by Sørensen[19]. The beams were designed for moment failure, hence the maximum shear force was considered to be the shear force occurring at expected moment failure.

Beam series M1 was designed with three reinforcement bars in a bundle. In design according to EC2 [8.9.1], this bundle can be assumed to act as one bar with an equivalent diameter, resulting in the same total area as the bundle. The necessary anchoring lengths were calculated according to EC2 [8.4] and the calculation sheet from Mathcad can be found in appendix 2. The calculated required anchoring lengths for the two beam types with bar reinforcement are presented in table 7.

	M2	M3
l_{bd}	150 mm	208 mm

Table 7: Required anchoring lengths

In the test setup, the free length outside each support was set to 300 mm, thus the anchoring capacity is satisfactory.

5.3.5 Summary

The six large beams with dimensions 200x300x4000 mm were to be tested in bending. The beams were divided into three differently reinforced beam types with two beams for each type. A 4-point bending test was chosen as a basis for the testing, with a

beam span of 3400 mm and with the jack load distributed as two load points placed with a 800mm distance between each other. The beams were calculated for moment resistance using both a simplified method and the multi-layer method. The shear resistance and the anchoring capacity were also controlled. The results from the design are shown in table 8 below:

Series	Rebars	Simplified $M_{simplified}$ [kNm]	Multi-layer $M_{multi-layer}$ [kNm]	Comparison $\frac{M_{multi-layer}}{M_{simplified}}$	Shear cap. V_{Rdc} [kN]	Failure load P_{Rd} [kN]
M1	3Ø12	55,96	56,94	1,018	113,75	87,60
M2	1Ø12	30,46	30,92	1,015	101,23	47,57
M3	none	14,4	16,62	1,154	72	25,57

Table 8: Calculation results

As can be seen from the results in table 8, the moment capacity is almost identical for the two different methods. This gives a good indication that no major calculation errors have been committed. The design failure loads are based on the moment capacity from the multi-layer method, as this is generally a more accurate approach. In this case however, it is of minor significance due to the similarity between the results.

As a result of the design, the final test setup and the cross section for each beam series are shown in figure 15.

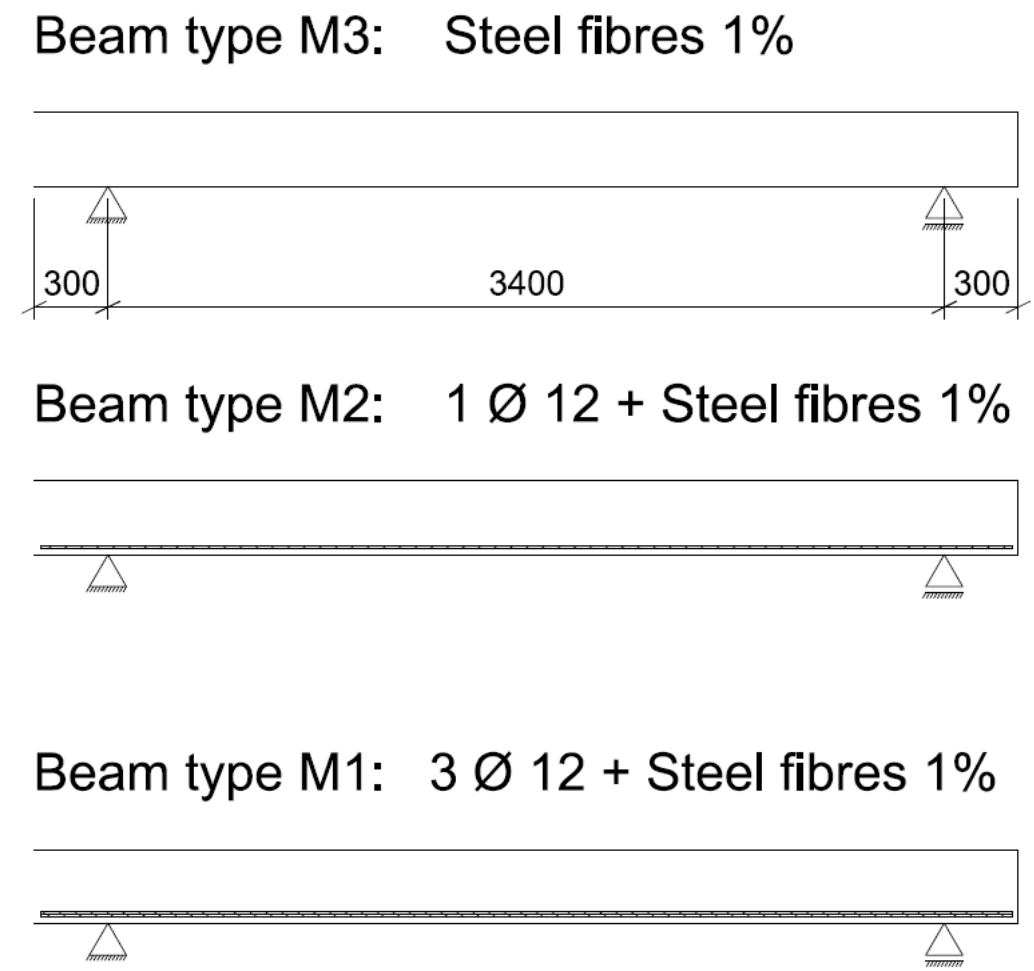

(a) beam types

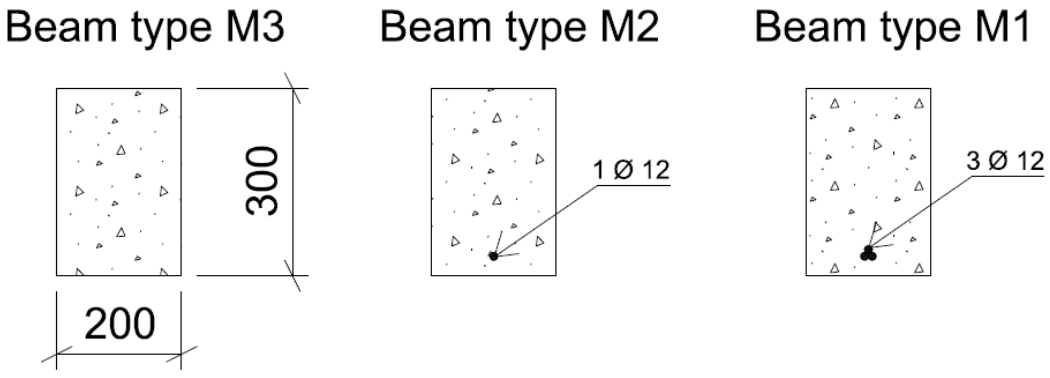

(b) cross-sections

Figure 15: Designed beam-types

Part III

Laboratory work

6 Casting Process

6.1 Concrete mixing

The concrete used in the casting was a self compacting concrete with a fibre amount of 1 vol%. The recipe (see appendix 4) was prepared by doctoral candidate G. Zirgulis, and the concrete was dimensioned as a B30, M60. The mixing was carried out at the Unicon concrete plant at Sluppen, and the fibres were added manually into the mixer. After mixing, the concrete was loaded on to a truck and transported to the NTNU lab for casting. Upon arrival at NTNU, a slump flow test was performed to check the flowability of the concrete. The test showed a flow diameter of approximately 380 mm. This was however not satisfactory, as the desired flow diameter of SCC is larger than 600 mm.[9] As a result, super plasticizer was added to the the mix to increase workability. This did increase the slump flow measure, but as a negative side-effect the concrete also started to show signs of segregation.

6.2 Casting of large beams

All the six large beams were cast with the same concrete mix. The concrete was poured from the truck into the formwork at one end, making the concrete flow to the other end more or less by itself. The high fibre amount of 1% reduced the workability of the concrete, and early in the casting process there was a problem with clustering in the funnel. After this was taken care of, the rest of the beams were cast without any further problems, and both the flow and fibre transportation seemed to be satisfactory when filling the formwork.

(a) casting procedure (b) concrete flow

Figure 16: Casting of large beams

6.3 Casting of standard beams and cubes

6.3.1 Standard beams

In addition to the six large beams, six standard beams were cast. These beams were cast according to NS-EN 14651[12]. The formwork was first filled in the middle, and then at the two ends. However, the concrete had already segregated in the wheelbarrow and as a result there was probably a somewhat higher intensity of fibres in the standard beams than in the large beams. The beams were to be tested according to the procedure described in 1.3.1 to determine the residual tensile strength of the fibre concrete.

Figure 17: Casting of standard beams

6.3.2 Cubes

Originally, six standard cubes were planned to be cast in order to determine the compressive strength of the concrete. However, only three cubes were cast due to

the poor condition of the concrete in the wheelbarrow. The cubes had to be leveled using the vibrating table because of the high fibre amount.

6.4 Testing of fresh concrete properties

I addition to the slump flow test, several other tests were performed to check the rheological properties of the fresh concrete. These tests were performed by another group simultaneously to the casting of the large beams.

6.4.1 4C-Rheometer

The test was performed as described in 2.3.1. It provides information about the yield stress and plastic viscosity of the concrete, that can be used to assess the risk of segregation and the flow capability. The results are presented in table 9.

Manually measured spread for correction	745 mm
Yield stress	12 Pa
Plastic viscosity	69 Pa·s

Table 9: Results from the 4C-rheometer

The results show a very low yield stress, and a moderate value for the plastic viscosity. Comparing to the diagram in figure 6 in section 2.3.1, these values indicate a substantial risk of segregation. Pictures from the test show a cluster of fibre and course aggregate in the centre of the spread, however the edge of the spread seems intact without bleeding. The moderate value of the plastic viscosity support the theory that adding super plasticizer affect the yield stress, but has minor effect on the plastic viscosity[20]. Also, the high spread diameter shows that probably too much plasticizer was added to the mix.

Figure 18: 4C-Rheometer Test

6.4.2 LCPC-BOX

The test was conducted according to the procedure in the article by N.Roussel[16]. However, the segregation in the concrete caused a bad flow in the box. As depicted in figure 19b, there is a fibre cluster at one end, while water and fine aggregate have spread a great length in the box. It therefore seems that the results from this particular test do not represent a realistic picture of the concrete properties. Although the concrete showed signs of segregation also when the large beams were cast, the flow was far better than the pictures from the LCPC-test show.

(a) Flow-spread

(b) Fibre cluster/segregation

Figure 19: LCPC-BOX test

6.4.3 Air content

The air content was measured using a specially designed 8 liter bucket with an air-tight lid. The special lid can be filled with water on top of the concrete, creating a water piston. A pump and a pressure gauge is mounted on top of the lid. When pumping, the concrete is compressed, and the change in volume can be measured as the air content. The result from the test showed an air content of 0,22%. This is a lower air content than what is normal for concrete. Considering that two other groups with similar concrete, measured an air content of 2-3%, it may be reasonable to assume that the measured value of 0,22% should have been higher.

Figure 20: Measuring the air content

6.5 Curing

One day after the casting, the concrete had set and the formwork was removed. The beams had nice smooth surfaces without any significant wounds. Some extra water was poured on the beam surfaces, and they were then covered by wet hessian sacks. Finally, the beams were wrapped in plastic to ensure a moist environment during the curing process. The beams cured for 35 days until the testing started.

(a) Removing the formwork (b) Curing environment

Figure 21: Curing of beams

6.6 Comments on the fresh concrete

When using self compacting concrete, the flowability is of major importance. Adding fibres to the concrete may reduce the workability if the dosage is too high, and this had to be taken into account when deciding the fibre content. In this thesis, the fibre content was set to 1-vol% in consultation with Terje Kanstad.

The fresh concrete was not as good as expected. Some problems occurred during the casting process, and there was early a problem with the concrete slump flow.

The reason for this was unknown, but as a measure to resolve this, superplasticizer was poured into the concrete mixer. The amount of plasticizer was probably too high and the concrete started to show signs of segregation afterwards. From the literature study, it is known that adding super plasticizer reduces the yield stress of the concrete, thus making it easier for the flow to start. However, the reduction of yield stress also increases the risk of segregation. In addition, studies suggest that adding super plasticizer has minor decreasing effect on the plastic viscosity[20]. With this in mind, the super plasticizer probably should have been added with more caution.

The other problem that occurred, was clustering of fibres in the funnel during casting of the large beams. This is known to be a potential problem when dealing with high fibre contents in the concrete. The Coin guidelines[5] refers to a "critical fibre amount" when using self compacting concrete. Exceeding this limit, may lead to fibre clustering. According to the product data sheet for Dramix 65/60, the recommended maximum dosage is 70 kg/m^3 for concrete with maximum aggregate size of 16 mm. The fibre amount of 1 vol% used in this concrete, is equivalent to a dosage of 80 kg/m^3. Based on this, using 1 % fibres may have been a bit ambitious with respect to a smooth casting process.

7 Testing of concrete elements

7.1 Testing of large beams

7.1.1 Preparation

The beams were placed in the test rig according to the decided test setup. The rig consisted of a rigid steel frame with a 1000 kN hydraulic jack, as depicted in figure 22. A steel beam was used to distribute the jack load into two point loads. Steel shims were used at support points to ensure good contact with the beam.

Figure 22: Test rig setup

A total of four inductive sensors (LVDTs) were attached to the beam at certain points at mid-span to measure strains and displacements during testing. The LVDTs were placed at the top, bottom, and at both sides at the height of the reinforcement bars. The sensors had a 2 Hz measuring frequency, meaning two registered points every second. All of the data points were logged by a computer, in order to create load-displacement diagrams and moment-curvature diagrams for the beams after testing.

LVDT	Type	Task
1	W10	Strain top
2	W10	Strain west side
3	W10	Strain east side
4	W100	Vertical displacement bottom

Table 10: Inductive sensors

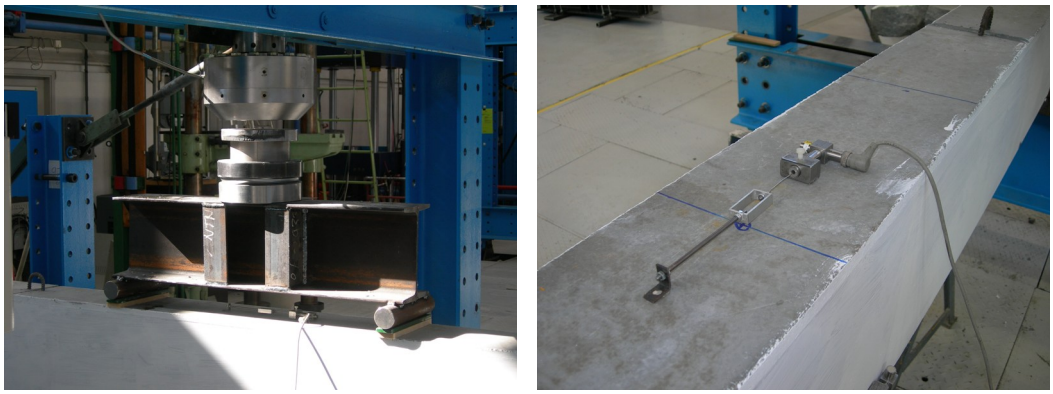

(a) load distribution beam (b) LVDT top

Figure 23: Testing details

7.1.2 Procedure

The jacks control unit was calibrated by the lab engineer. The jack was set to induce a vertical displacement of 2 mm per minute for the two beams with only fibre reinforcement, and 3 mm per minute for the beams with additional reinforcement bars. The test was divided into load steps, where the jack was stopped and the development of cracks was examined. In the first step, the load was increased until the first indication of cracks could be seen. After this, the jack was stopped at increasing loads of 10 kN to register crack distribution and widths, until failure occurred.

7.1.3 Crack registration

For each load step, the development of cracks was marked and crack widths were measured. The main registration of cracks was done at a load step corresponding to approximately 50% of the beams capacity to simulate the situation in serviceability limit state (SLS). Here, the crack widths were thoroughly measured using a special binocular and the mean distance between the cracks was calculated.

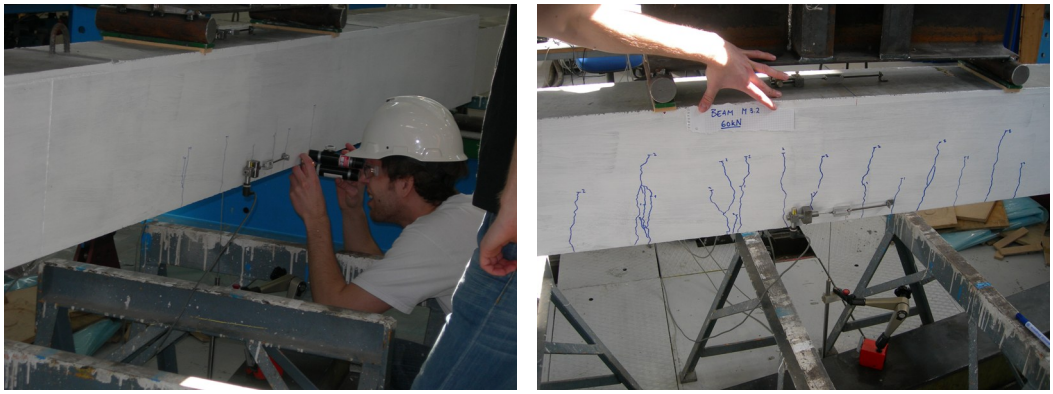

(a) measuring crack widths (b) crack development

Figure 24: Registration of cracks

7.2 Testing of standard beams

The standard beams were tested in bending as described in chapter 1.3.1, in order to determine the flexural tensile strength of the concrete. The 25 mm sawed notch at mid-span was made on the side of the beam relative to the casting orientation. This was to reduce the effect of the favourable fibre orientation in the bottom due to the casting procedure. The exact height and width of the beams were measured with a digital vernier caliper to be used in the calculations. Inductive sensors were attached to the beam in order for a computer to monitor the load-deflection relation. The test situation is depicted in figure 25.

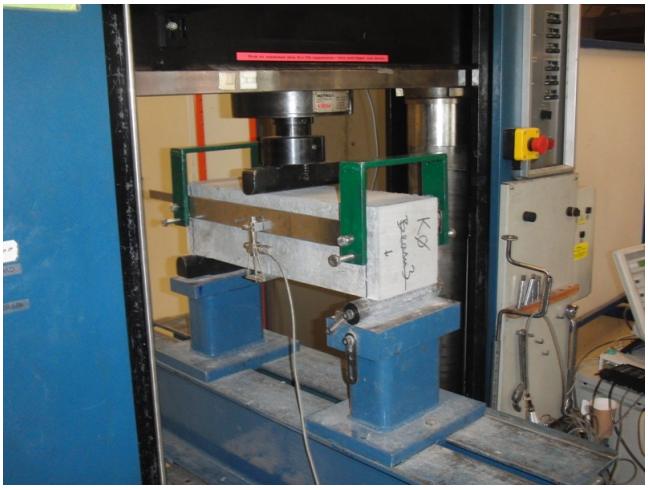

Figure 25: Testing of standard beams

7.3 Testing of cubes

The three cast cubes did as mentioned contain a higher amount of fibres than what is representative for the large beams. They were nevertheless tested in the laboratory

by the lab engineers to estimate the compressive strength. The cube strength $f_{ck,cube}$ found from testing can be converted to the cylinder strength f_{ck} to be used in the calculations.

Part IV

Results and discussion

8 Standard beams and cubes

8.1 Standard beams

The data from the standard beam test were processed in an excel-spreadsheet by B. Fernadez. Beam 5 had very irregular results due to a problem with the LVDTs, and the results from this beam was excluded. The diagram in figure 26 shows that all the beams had the expected ductile behaviour. The load increased even after cracking occurred, thus hardening behaviour is satisfied. Moreover, the beams had more or less similar strength. The only exception was beam 1, which had a slightly higher capacity.

The parameter of most interest is $f_{R,3}$, which is used to calculate the residual tensile strength $f_{ftk,res2,5}$.

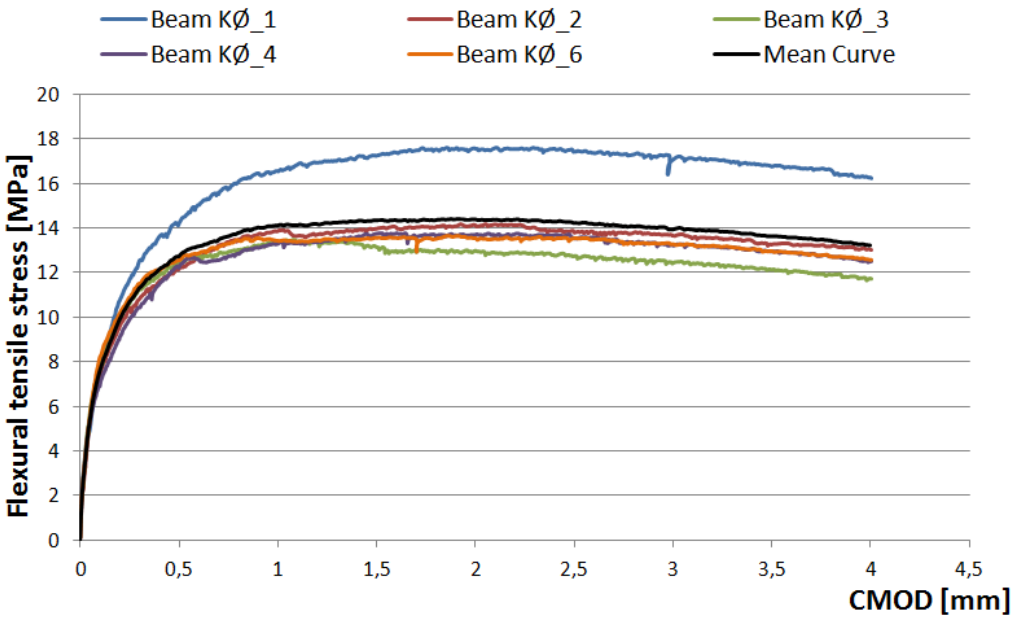

Figure 26: $f_{r,i} - CMOD$ diagram from testing of standard beams

Beam	1	2	3	4	5	6	Mean Value
$f_{R,3}[N/mm^2]$	17,6	14,1	12,8	13,7	-	13,5	14,8

Table 11: Values for $f_{R,3}$ from testing of standard beams

$f_{ftk,res2,5}$ is found by multiplying the mean value for $f_{R,3}$ by 0,37 according to the expression in 1.3.1. This gives the following value for the residual tensile strength based on the testing:

$f_{ftk,res2,5} = 5,49 N/mm^2$

Due to the problems described in section 8.1 during casting of the standard beams, it may be reasonable to assume that this value is too high to be representative for the large beams. However, no fibre counting was conducted to confirm this suspicion, and thus the assumption can not be conclusive.

8.2 Cubes

The three standard cubes were tested by the lab engineers. The measured cube compressive strength is presented in table 12 below:

	C1	C2	C3	Mean value
$f_{c,cube}$[MPa]	75	75	71,2	73,7

Table 12: Compressive cube strength

The characteristic cylinder strength f_{ck} for concrete should usually be based on the statistical 5%-fractile value from major scale testing, meaning that 95% of the tested specimens have higher compressive strength than the characteristic value. In this thesis, the compressive strength is taken as the mean value from three tested cubes and can strictly speaking not be defined as the characteristic strength. Still, it is chosen to denote it f_{ck}, since this is the common term for the compressive strength. To find the cylinder compressive strength, the mean value of the cube strength was multiplied with the factor 0,8. This gave the following value:

$f_{ck} = 59,0$ MPa

The concrete was proportioned as B30, and the value of 59,0 MPa is certainly higher than what was expected. However, the cubes were tested approximately 50 days after casting instead of the standard 28 days. This extra curing time has probably contributed to a higher compressive strength.

9 Moment

During testing of the full scale beams, several factors were measured and registered; Time, jack-load, displacement at midpoint, strain on top of the beam and strain at the sides. The data were used to find the capacity of the cross section and to show the behaviour of the beams in bending. The beams were loaded until failure occurred. After the beams had reached maximum load, the jack was run even further to monitor the ductile behaviour.

Calibration error of the jack

During testing, the first beams seemed to withstand a much higher load than expected based on the calculations made prior to the testing. The first test beam, beam M3.2, failed at a loading almost three times higher than the estimated failure load. It was expected that the calculations would not be exact, since the residual tensile strength used in the pre-calculations was an assumed value based on previous experiments. However, this major difference was strange. The lab engineer helping with the testing, later found out that the load-jack was not properly calibrated and that the load registered by the testing equipment was to large. To get the correct values, the jack load had to be multiplied with a factor $\frac{2}{3}$. As a result, all capacities and plots made in the following chapters are multiplied with this factor to get the correct load values.

9.1 Load-displacement

To visualize the behaviour of the beams during testing, load-displacement diagrams were made from the registered data points. The measured vertical displacement at midpoint and the corresponding jack load are plotted together.

9.1.1 Beam series M1

Beam	P_{max} [kN]	$\delta_{P,max}$ [mm]
M1.1	113,19	23,38
M1.2	109,51	20,20

Table 13: M1 - maximum load and corresponding displacement

The two beams showed similar behaviour with respect to both deflection and maximum load capacity. The beams sustained high capacity also after maximum load was reached, thus both beams has a ductile failure behaviour. Beam M1.1 was

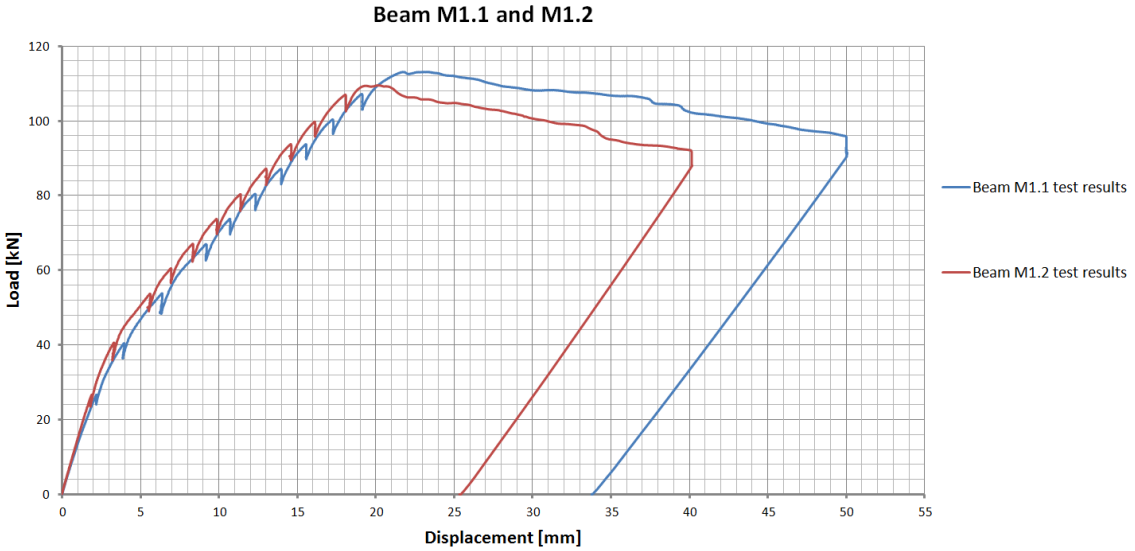

Figure 27: Load-displacement diagram for beam series M1 based on test results

loaded until the deflection at midpoint was 50 mm with a corresponding 97 kN jack load. Testing of beam M1.2 was stopped at 40 mm deflection and 92 kN jack load. At 40 mm displacement, the jack load on beam M1.1 was 102,5 kN. The capacity of the beams at 40 mm displacement had dropped 9,4 % for M1.1 and 15,8 % for M1.2.

9.1.2 Beam series M2

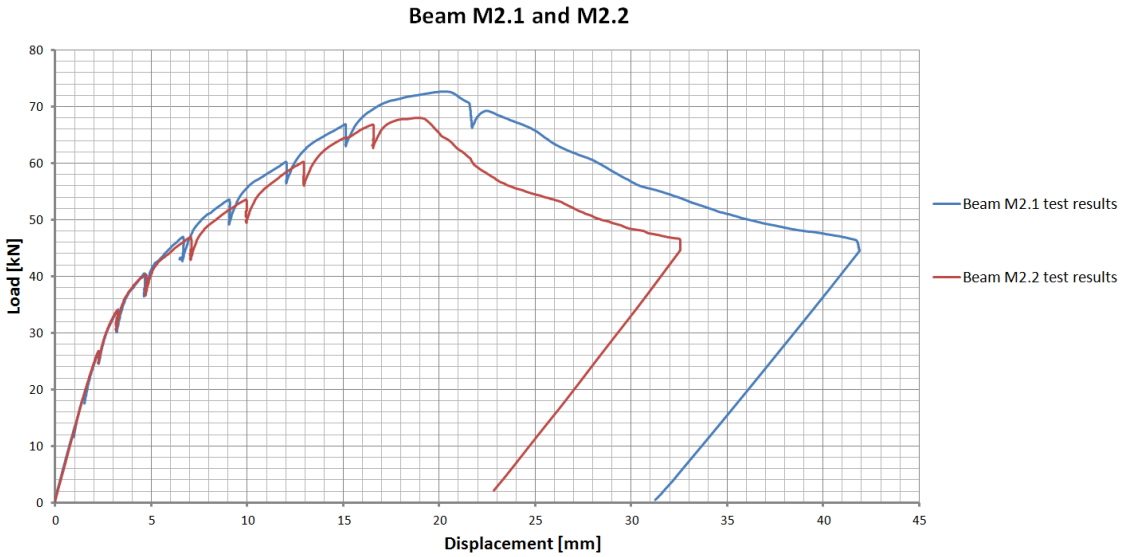

Figure 28: Load-displacement diagram for beam series M2 based on test results

Beam	P_{max} [kN]	$\delta_{P,max}$ [mm]
M2.1	72,72	20,43
M2.2	68,03	18,92

Table 14: M2 - maximum load and corresponding displacement

The two beams in series M2 also had similar behaviour, and both showed a ductile failure. However, they did not maintain the capacity after failure to the same extent as beam series M1. Beam M2.1 was loaded until the jack load was reduced to 47 kN with a displacement of 42 mm. Beam M2.2 was loaded to 47 kN and a displacement of 33 mm.

9.1.3 Beam series M3

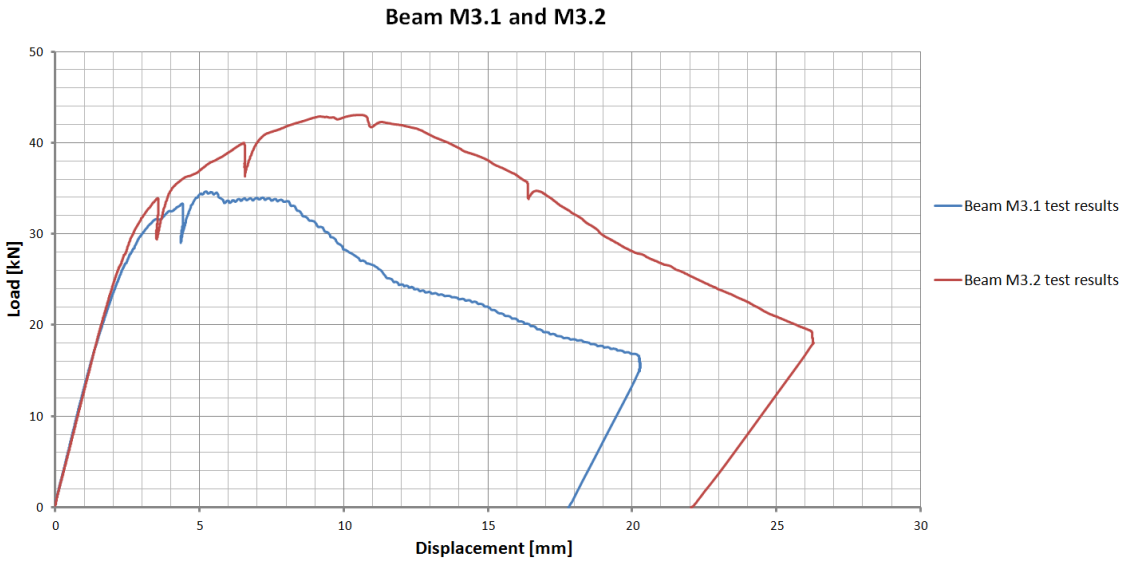

Figure 29: Load-displacement diagram for beam series M3 based on test results

Beam	P_{max} [kN]	$\delta_{P,max}$ [mm]
M3.1	34,65	5,26
M3.2	43,06	10,66

Table 15: M3 - maximum load and corresponding displacement

This beam series did not have any bar reinforcement, only fibres. The total capacity was lower and the beams failed at lower displacements than the other series. Nevertheless, the loading could be increased after cracking occurred, thus hardening behaviour is satisfied. The failure was also ductile for both beams. The difference in maximum load and maximum displacement between the two beams M3.1 and M3.2 were also higher than for the other series. Beam M3.2 have 24,3 % higher load

capacity, and the maximum load occurred at a displacement 103 % higher than for beam M3.1.

9.1.4 Summary

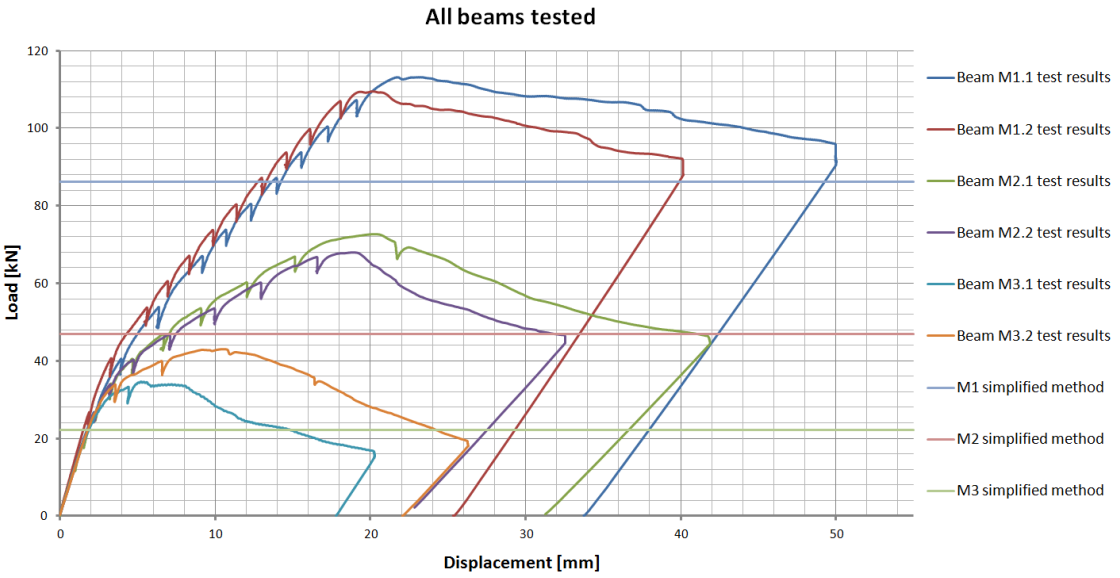

Figure 30: Load-displacement all beams

In figure 30, the load-displacement curves for all the beams are shown together with the calculated capacities from the simplified method shown in section 5.3.2. The calculations made with the simplified method used the planned material data for a B35 concrete and a residual tensile strength $f_{ftk,res2,5} = 2,0MPa$. As can be seen from the plot, the capacities for all the beams are higher than the calculated values. This indicates that the fibre contribution is greater than the assumed value of $f_{ftk,res2,5} = 2,0MPa$.

9.2 Concrete strains

Figure 31 and 32 show the measured strains on the beams plotted against the jack load during testing. The tensile strains at the sides were measured with two LVDTs, one on each side of the beam, placed at the same height as the bar reinforcement. Compressive strain top was measured with a LVDT placed on the topside of the beam.

The strain plots show how the middle of the beam behaves during loading. The measurements are accurate if the crack development is uniform along the beam length and no large cracks occur outside the LVDTs measuring length. Based on the strain plots, the strain measurements seem to be reasonable compared to the

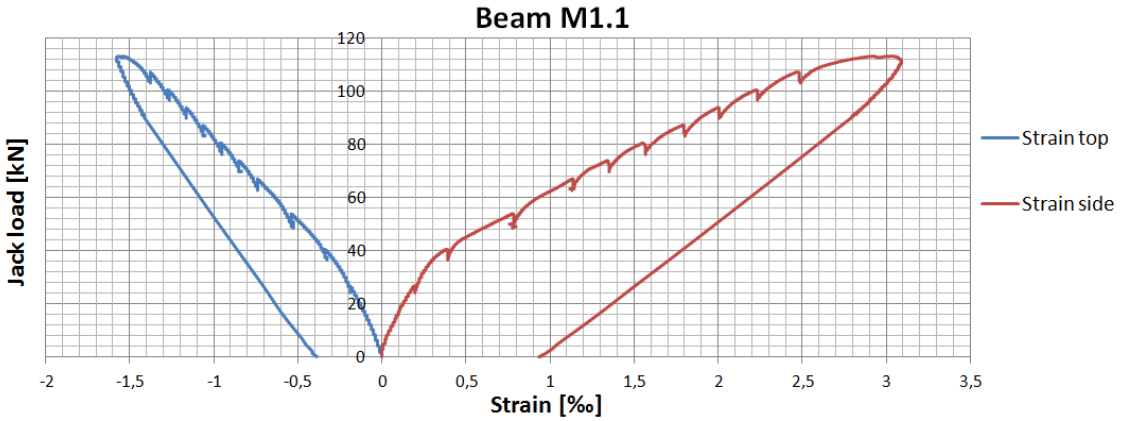

(a) M1.1

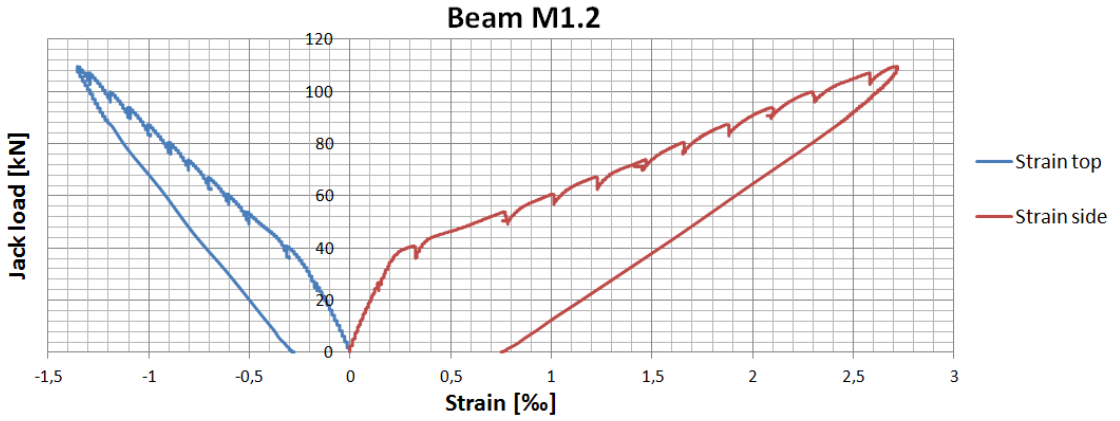

(b) M1.2

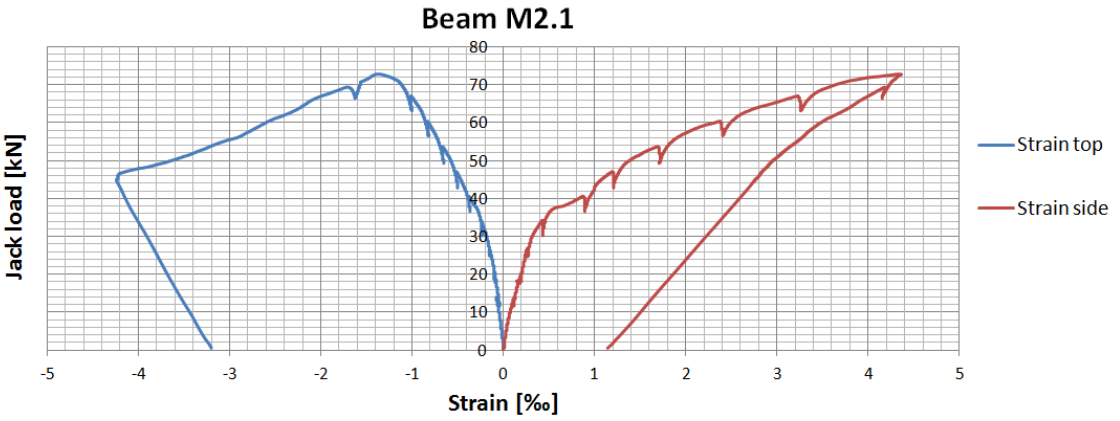

(c) M2.1

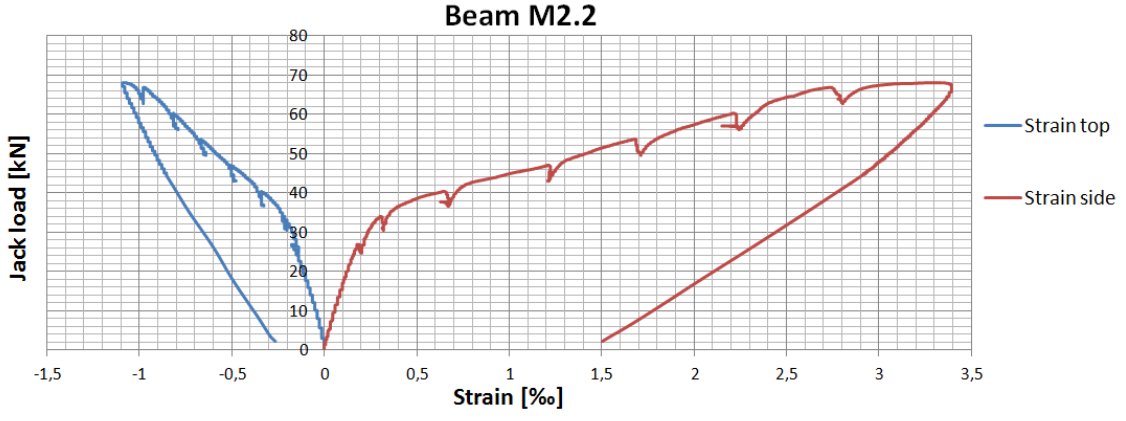

(d) M2.2

Figure 31: Concrete stains during testing, series M1 and M2

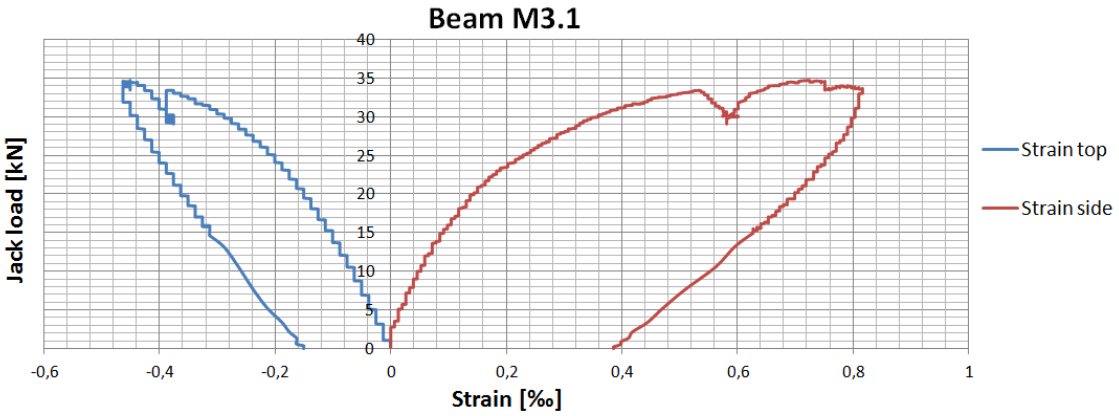

(a) M3.1

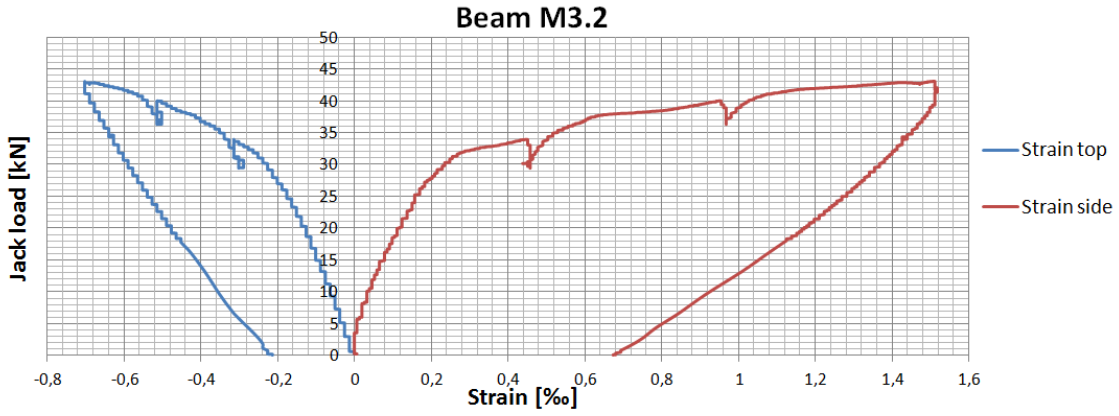

(b) M3.2

Figure 32: Concrete stains during testing, series M3

load-displacement plot by looking at how the graphs develop, and where the halts from the load steps are located on the curves. When the beams fail, the comparison between the load-displacement curves and the strain curves becomes inaccurate. When the main failure crack develops, strains are allocated to the main crack and the strain measurements are dependent on the location of the crack. The main failure crack occurred outside the strain measuring length on five out of the six beams. On these five beams, the strains halted at the maximum value until the beams were unloaded. Beam M2.1 developed the main failure crack at the middle of the beam. The crack started outside the side LVDT's in the bottom of the beam, but developed upwards inside the measuring length of the LVDT on top of the beam. This can be seen in the strain plot in figure 31c for beam M2.1, where the compressive strain in the top increased after the beam had failed.

9.3 Moment capacity

9.3.1 Moment-curvature relationship

In order to visualize the moment development in the beams from the test data, it is appropriate to establish a moment-curvature diagram. The curvature of the beams could be calculated based on the strain measurements registered by the LVDTs. In this case, the formula for curvature could be expressed as:

$\kappa = \frac{\varepsilon_{b,mean} - \varepsilon_{top}}{d}$

This method only takes into account the strains/cracks between the two measure points of the LVDTs. If large cracks occur outside the measuring points, the calculated curvature becomes inaccurate. A better way of describing the curvature of the beams is to develop a relation between the displacement at mid span and the beam curvature. The relation can be found using the unit load method based on the principle of virtual forces. The relation between displacement and curvature can be expressed as:

$$\delta = \int_L \frac{M(x)}{EI} \cdot \widetilde{M}(x) \cdot dx = \int_L \kappa(x) \cdot \widetilde{M}(x) \cdot dx$$

To solve the integral, tabulated solutions are used. The tabulated solutions use the diagrams for curvature and virtual moment. The virtual moment diagram is found by putting a unit load at the midpoint of the beam, which gives a triangular moment diagram with maximum value $\widetilde{M} = \frac{L}{4}$. The curvature diagram is found by assuming constant relationship between moment and curvature. The curvature diagram is then the same as the moment diagram for our beam setup, with a maximum value of κ_0 between the two load points. By using the tabulated solutions for the integral, the expression for the displacement can be written as:

$$\delta = \frac{349}{3468} \cdot \kappa_0 \cdot L^2$$

Which gives the relation between displacement and curvature:

$$\kappa = \frac{3468}{349} \cdot \frac{\delta}{L^2} \approx 9,94 \cdot \frac{\delta}{L^2}$$

were

δ =Vertical displacement measured at mid span

L =Beam span

By using the test data as input in this expression, the curvature can be calculated and the moment-curvature plot can be established. The complete calculation is shown in appendix 3.

9.3.2 Moment-curvature diagrams

The moment-curvature diagram for each beam was calculated and plotted based on the derived expression in the previous section.

From testing of standard beams and cubes, the concrete compressive strength f_{ck} and the residual tensile strength $f_{ftk,res2,5}$ were determined to be $f_{ck} = 59MPa$ and $f_{ftk,res2,5} = 5,49MPa$. These values were much higher than expected, but to see if they were representative also for the large beams they were used as input values in the multi-layer simulation.

A multi-layer simulation with the assumed values before testing was also run, and a moment-curvature diagram was plotted. Contrary to the values from the standard beam test, these values were assumed to be lower than the actual behaviour of the beams based on the load-deflection diagrams.

In the next sections, the three graphs are plotted in the same diagram for comparison:

- Values from the standard beam and cube test, $f_{ck} = 59MPa$ and $f_{ftk,res2,5} = 5,49MPa$
- Assumed values before testing, $f_{ck} = 35MPa$ and $f_{ftk,res2,5} = 2MPa$
- Actual behaviour based on the large beams test data

9.3.3 Series M1

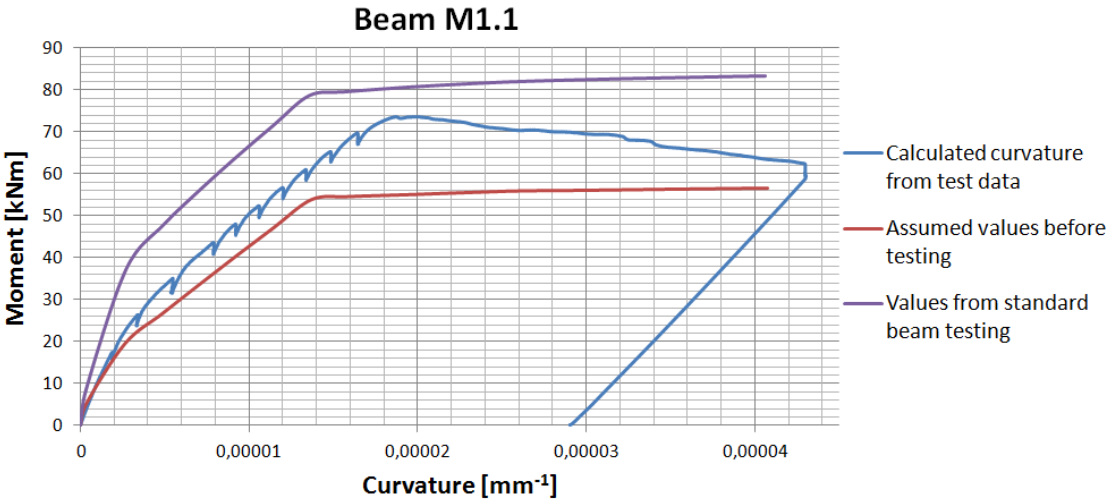

Figure 33: Moment-curvature Beam M1.1

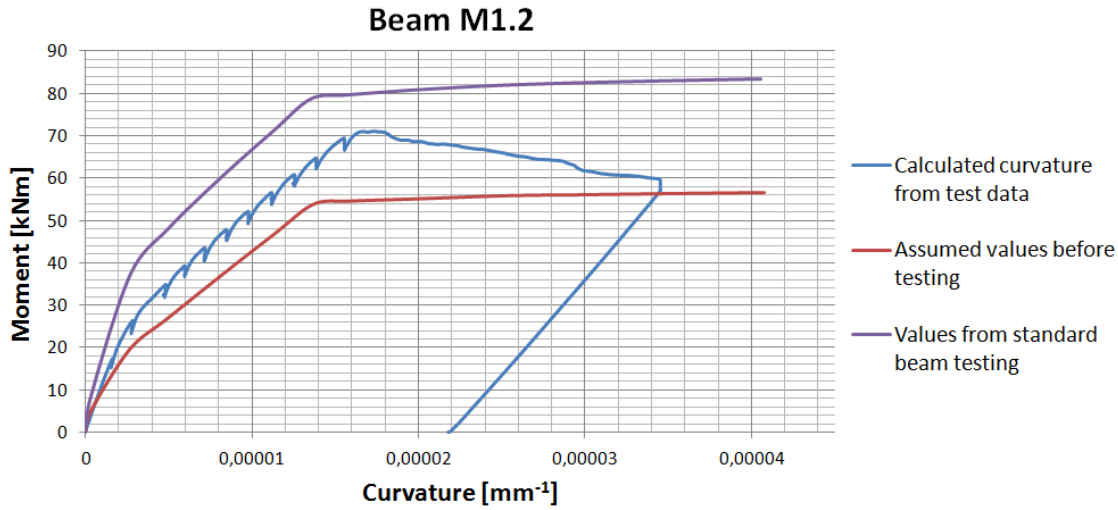

Figure 34: Moment-curvature Beam M1.2

From the testing of the full scale beams, the following moment capacities were measured:

- Beam M1.1: $M_{Rd,test} = 73,57kNm$
- Beam M1.2: $M_{Rd,test} = 71,18kNm$

By using the measured compression strength from the cube testing, and the measured residual tensile strength from the standard beam test, the calculated moment capacity in the multi-layer method was too high. With $f_{ck} = 59MPa$ and $f_{ftk,res2,5} = 5,49$, the moment capacity of this cross section is $M_{Rd,design} = 83,40kNm$.

For concrete with a compressive strength above 50 MPa, the tensile strength of the concrete before cracking was calculated according to EC2 table 3.1:

$$f_{ctm} = 2,12 \cdot \ln(1 + \frac{f_{ck}+8}{10})$$

With a compressive strength of $f_{ck} = 59MPa$, the tensile strength is $f_{ctm} = 4,33MPa$.

From the pre calculations with $f_{ck} = 35MPa$ and $f_{ftk,res2,5} = 2,0MPa$, the moment capacity was $M_{Rd,pre} = 56,94kNm$.

9.3.4 Series M2

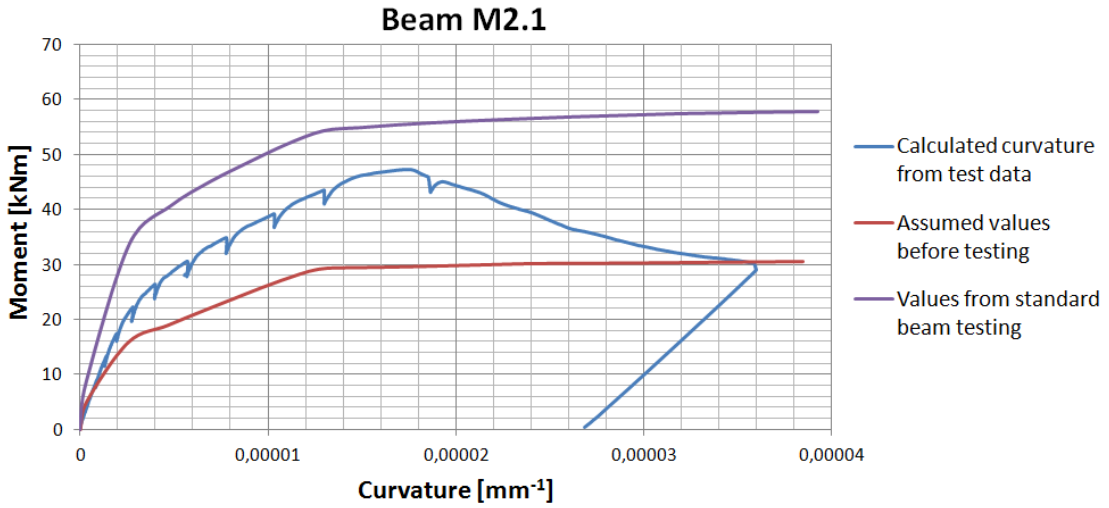

Figure 35: Moment-curvature Beam M2.1

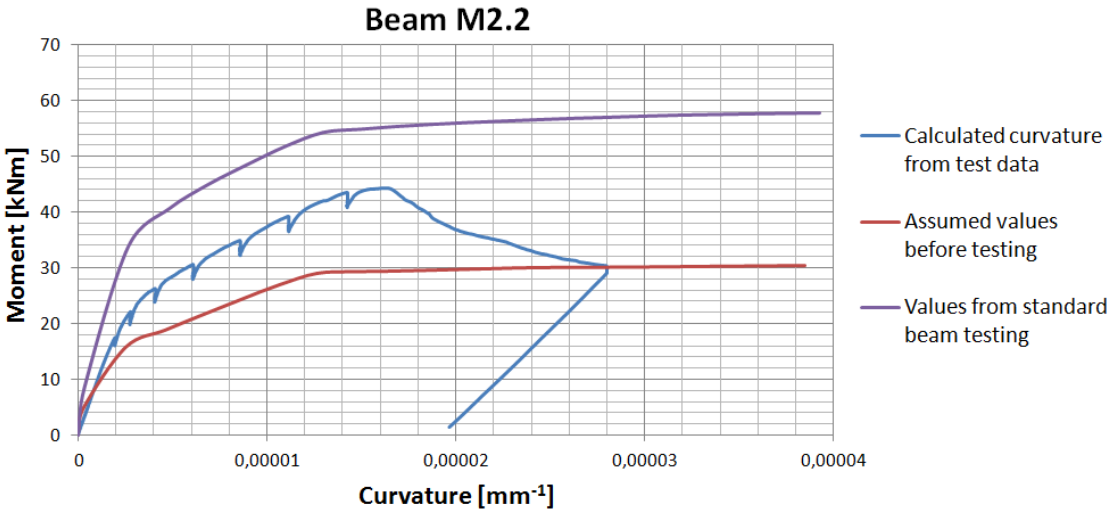

Figure 36: Moment-curvature Beam M2.2

Maximum measured moments in test series M2:

- M2.1: $M_{Rd,test} = 47,27kNm$
- M2.2: $M_{Rd,test} = 44,22kNm$

The beams behaved similar up to about 30 kNm where beam M2.1 had a bit steeper moment development and a higher maximum capacity. The multi-layer pre-calculation gave a moment capacity of $M_{Rd,pre} = 30,92kNm$. The capacity with the values from standard beams was calculated to $M_{Rd,design} = 57,72kNm$. The beam series M2 have, similarly to beam series M1, a lower measured capacity than the calculated capacity from the standard beam test data.

9.3.5 Series M3

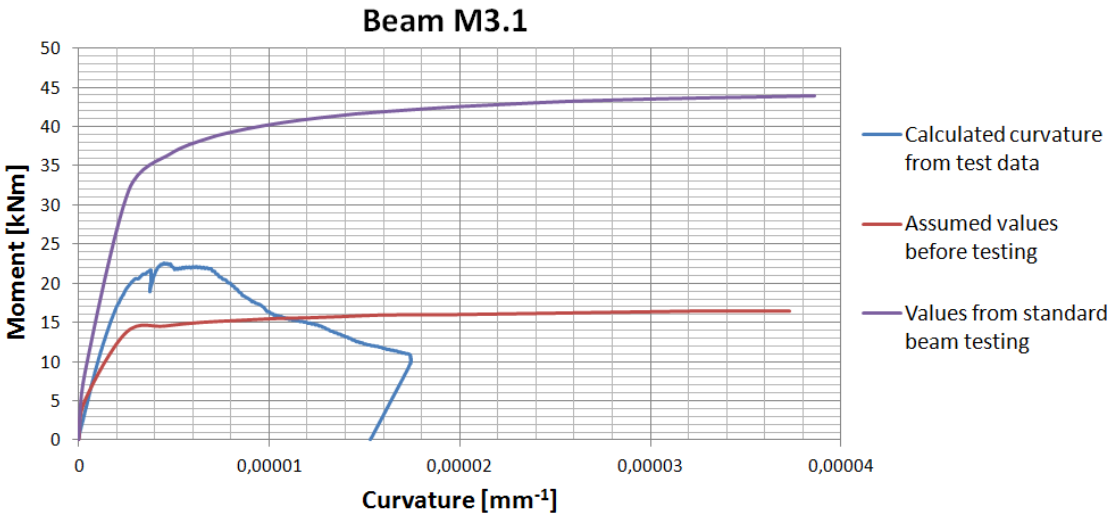

Figure 37: Moment-curvature Beam M3.1

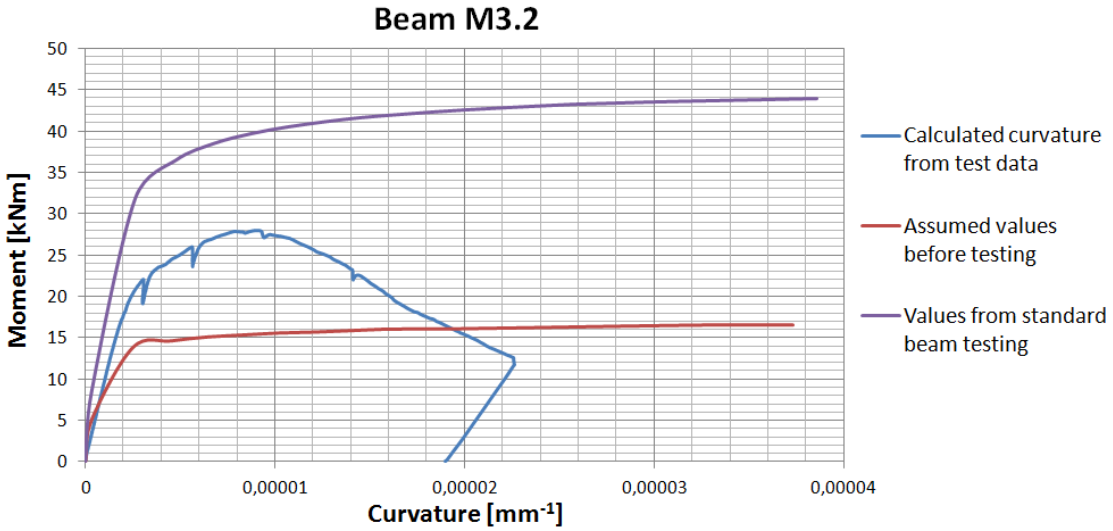

Figure 38: Moment-curvature Beam M3.2

Maximum measured moments in test series M3:

- M3.1: $M_{Rd,test} = 22,52kNm$
- M3.2: $M_{Rd,test} = 27,99kNm$

The two beams in test series M3 had a larger spread in the measured data than the other test series. The pre-calculation gave a capacity of $M_{Rd,pre} = 16,62kNm$ and the measured data gave a capacity of $M_{Rd,design} = 43,99kNm$.

9.3.6 Discussion

All of the moment-curvature diagrams show the same tendency; neither the values from the standard beam test nor the values assumed before testing fit the actual behaviour of the large beams. The values from the standard beams resulted in a too stiff behaviour and too high moment capacity, while the pre-assumed values gave a too low capacity. In the simulations, the residual tensile strength has more influence on the moment capacity than the compressive strength. This indicates that the actual fibre contribution $f_{ftk,res2,5}$ in the large beams is somewhere between these two states. Beam series M1 and M2 had a behaviour closer to the curve with values from standard beam testing, while the beams without bar reinforcement in series M3 lie closer to the pre-testing curve. To find an estimate for the actual fibre contribution, a curve that better matches the test results needs to be established. This was performed as described in the next chapter.

9.3.7 Curve fitting

To find a curve that matched the behaviour of the beams in testing, several simulations were run using the multi-layer program in excel. To find a fitting curve, the residual tensile strength was used as an unknown factor. $f_{ftk,res2,5}$ was put into the multi-layer program with different values until the capacity calculated by the program matched the capacity measured in the beam test. Since each beam series includes two similar beams, the curve fitting was made so that it matches the average value of the two beams in each series.

Series M1

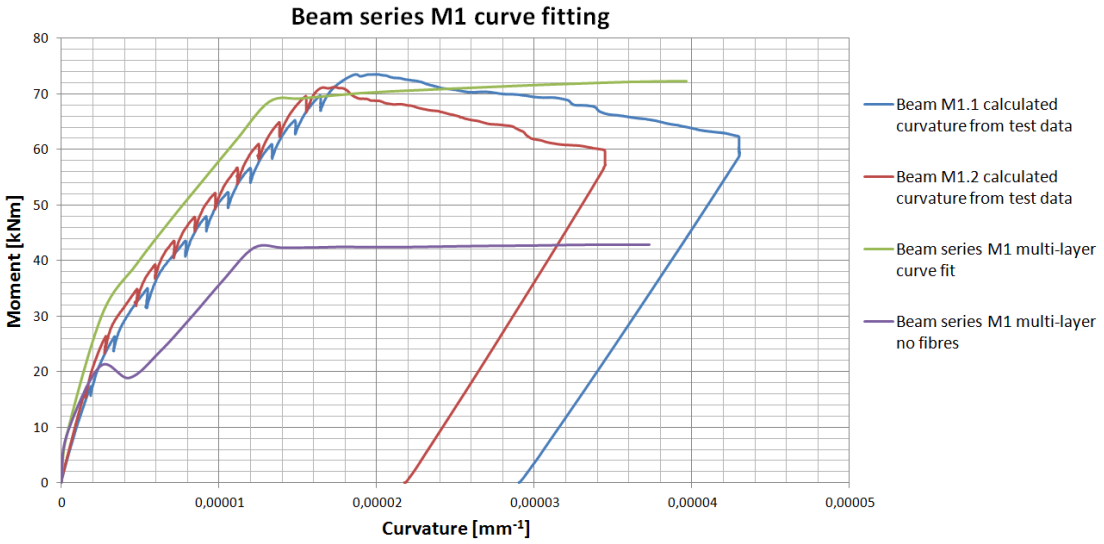

Figure 39: Beam series M1 curve fit with adjusted $f_{ftk,res2,5}$

To make the multi-layer method curve match the tested beams, $f_{ftk,res,curvefit} = 3,9MPa$ was found to be the best value. These values gave a calculated moment capacity of $M_{Rd,curvefit} = 72,34kNm$, which is approximately the mean value of the tested moment capacities of the two beams in series M1. The residual tensile strength of the adjusted curve was 40 % lower than the measured value form the standard beam test. Even though the curve fit matched the moment capacity of the tested beams, the simulation gave a stiffer behaviour than the test results until failure occurred.

Series M2

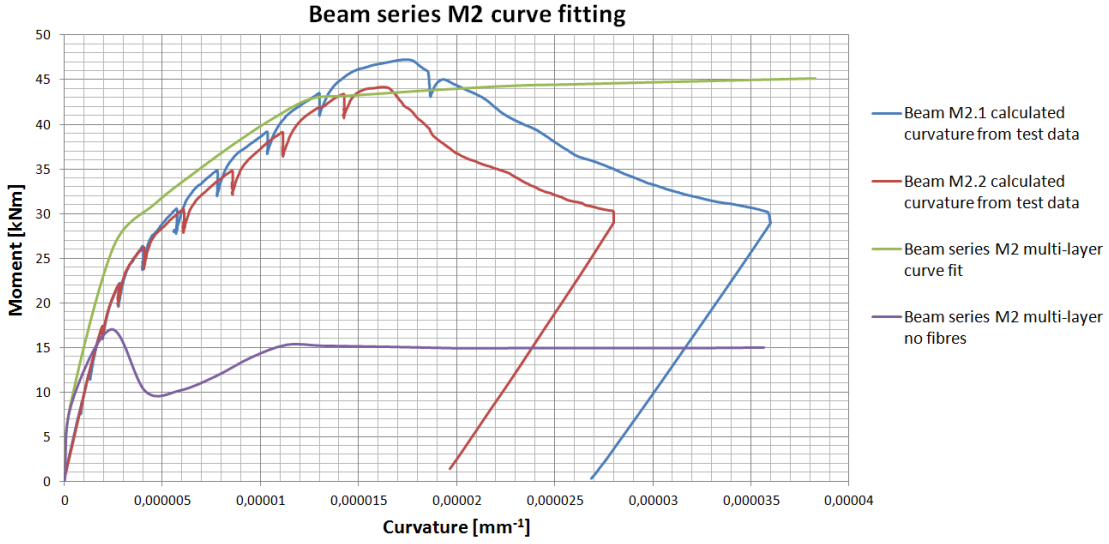

Figure 40: Beam series M2 curve fit with adjusted $f_{ftk,res2,5}$

To make the calculated values fit the measured data, a curve fit with $f_{ftk,res,curvefit} = 3,8MPa$ was used. This value was almost the same as the curve-fit value in series M1. The calculated capacity then became $M_{Rd,curvefit} = 45,16kNm$. Also for this series, the adjusted curve had a stiffer behaviour before failure than the test curves. For the beams in series M2 the adjusted residual tensile strength of 3,8MPa is 44,5% lower than the tested residual tensile strength of 5,49MPa.

Series M3

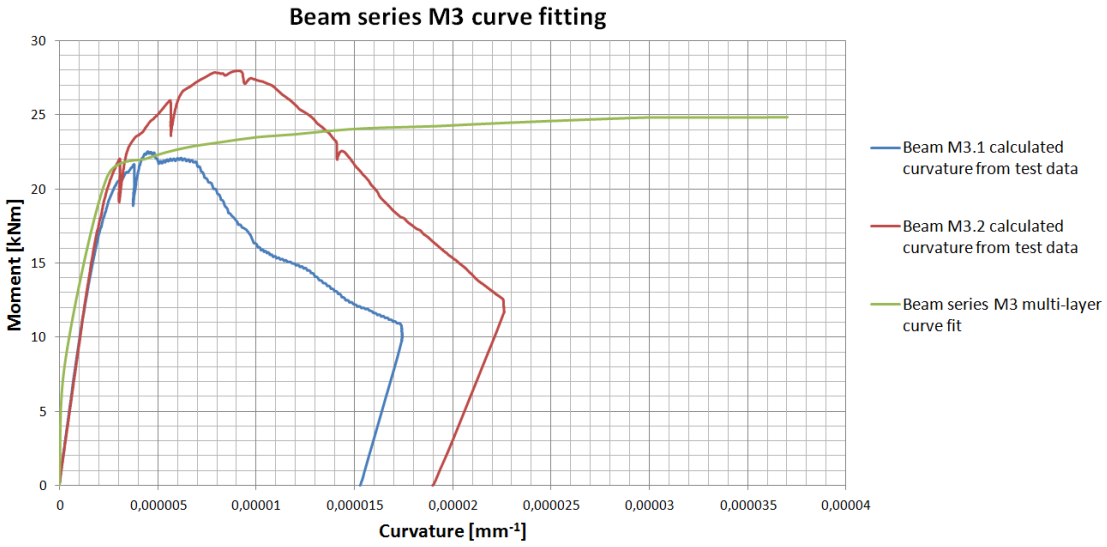

Figure 41: Beam series M3 curve fit with adjusted $f_{ftk,res2,5}$

In the curve fit of series M3, a residual tensile strength value of $f_{ftk,res,curvefit} = 3,0MPa$ was used. This value is significantly lower than for the two other series. The adjusted residual tensile strength of 3,0MPa is 83% lower than the measured value of $f_{ftk,res2,5} = 5,49MPa$. The capacity with the adjusted value was $M_{Rd,curvefit} = 24,83kNm$.

Comments on the curve fitting

By running simulations in the multi-layer program in excel with $f_{ftk,res2,5}$ as a variable parameter, it was possible to establish curves that matched the actual moment capacity of the beams during testing. The residual tensile strength used to create these curves can be assumed to represent the actual fibre contribution in the large beams. The adjusted residual tensile strength from the curve-fitting are summarized below.

Beam series	$f_{ftk,res,curvefit}$ [MPa]
M1	3,9
M2	3,8
M3	3,0

In the beam series with bar reinforcement, series M1 and M2, the adjusted values for the residual tensile strength were almost the same, while the beam series with no bar reinforcement had a lower value. The reason for the higher residual tensile strength in the beams with bar reinforcement could be a more favourable fibre distribution. The self-compacting concrete was cast from a stationary point at one end of the formwork. When the concrete was flowing from the casting point towards the other end, the bar reinforcement in the bottom of the formwork could make the fibres align parallel to the bars. With more fibres parallel to the bar reinforcement, the tensile strength contribution from the fibres increases.

Even though the fitted curves match the maximum moment capacity of the tested beams, they do not represent the actual beam behaviour after the maximum load has been reached. The capacity of the tested beams gradually decreases for increasing deflection after maximum load, while the straight line on the simulation curves suggests that the capacity would be sustained. The reason for this is that the multi-layer simulation assumes an evenly plastic distribution of strains along the beam length. However, for the tested beams the strains will allocate to the main crack after maximum load is exceeded, resulting in a hinge. Hence the capacity will decrease.

9.3.8 Fibre contribution

For beam series M1 and M2, calculations with the multi-layer method disregarding the fibre contribution were also preformed. These were made to show how much the fibres contribute to the moment capacity of the beams. The graphs in figure 39 and 40 show the theoretical behaviour of the beams without fibres. The graph without fibres was compared to the curve-fit graph. The difference in capacity between the graphs represents the fibres contribution to the moment capacity. The calculations have the larges moments at the strain limit of $\varepsilon_{uk} = \frac{3}{h} = 10‰$, thus the comparison was performed at this state.

The moment capacities at $\varepsilon_{uk} = 10‰$ in the calculations without fibres are:

$$M_{1,nofibre} = 42,95kNm$$
$$M_{2,nofibre} = 15,02kNm$$

The theoretical contribution from the fibres can then be calculated:

$$M_{1,fibre} = M_{1,Rd,curvefit} - M_{1,nofibre} = 29,39kNm$$
$$M_{2,fibre} = M_{2,Rd,curvefit} - M_{2,nofibre} = 30,14kNm$$

9.3.9 Discussion of the moment capacity

Ductility

The load-displacement diagrams made using the test data for the large beams in section 9.1 show how the beams behaved during bending. After failure, all the beams gradually reduced the loading resistance with increasing displacements. There was no sudden drop in capacities, thus all the beams demonstrated a ductile behaviour. The beams with bar reinforcement combined with fibres, series M1 and M2, reached failure load at approximately 20 mm displacement at the midpoint, while the beams with only fibres reached their maximum load capacity at lower deflections. The descending load-displacement curve after failure had least slope for beam series M1, the series with most bar reinforcement. This indicates that for the concrete, and the fibre amount used in this thesis, the ductility increases with increasing amount of bar reinforcement. However, all the tested beams with bar reinforcement are under reinforced, so the assumption may not be valid for beams with higher bar reinforcement ratio.

Residual tensile strength

The test results show that the residual tensile strength of the fibres had profound effect on the moment capacity of the large beams. In the preparation and design of the large beams, the value of the residual tensile strength was assumed to be $f_{ftk,res2,5} = 2,0MPa$. This value was based on previous studies and testing and it was expected that this value would not be exact. The standard beam test determined the value to be $f_{ftk,res2,5} = 5,49MPa$. As discussed in section 8.1, this value was probably to high and when used in calculations it did not match the results from the large beam testing.

When comparing the simulation without fibres with the test curves in the moment-curvature diagrams in figure 39 and 40, it can also be seen that the fibres influence the stiffness in the transition before and after cracking (Stage I and II). The simulation without fibres get a sudden drop in stiffness when the concretes tensile strength is exceeded and the stress is transferred to the reinforcement bars. The curves with fibres have a smoother transition, and the capacity increases evenly after cracking. From this it can be assumed that the fibres ability to transfer stress across the cracks contributes to sustain the stiffness between state I and II better than for a conventionally reinforced beam.

9.4 Failure modes

During the large beam testing some observations were made. The test setup chosen, with a four point bending solution, should theoretically make the beams fail in bending at a random location where the concrete is weakest within the constant maximum moment area. All the beams failed in bending as expected, but five out of six beams failed at the same location along the beam span outside the maximum moment area as shown in figure 42.

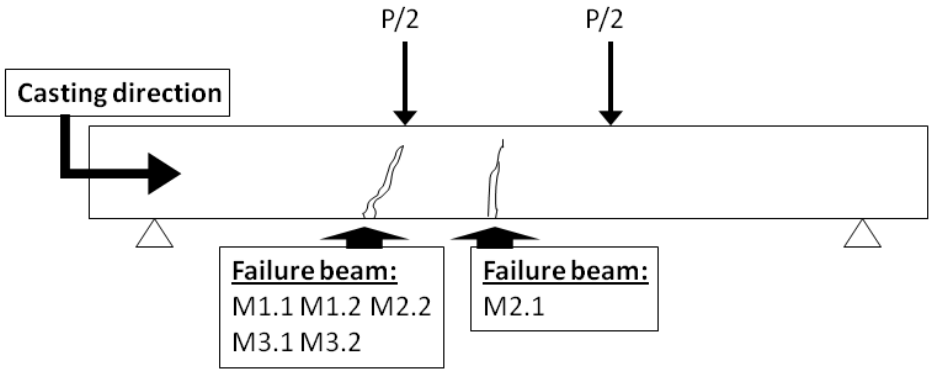

Figure 42: Failure of large beams

The common failure in five of the six beams started as a crack outside the maximum moment area and spread inclined towards the nearest loading point. Beam M2.1 had a more expected failure, with a crack forming inside the maximum moment area. The main crack for the five beams with same failure pattern all occurred under the load point closest to the side the concrete was cast from.

The fact that five out of six beams failed in the same location is probably not coincidental. A possible explanation could be that the concrete flow during casting had an uneven transportation of fibres along the beam length. This may have lead to a lower fibre amount in certain areas resulting in a weaker cross-section. This could have been investigated further by performing a fibre counting in different cross-sections after testing. However, this was not done and it was not confirmed that the fibre amount was lower in the failure area.

Another possible reason could have been a minor imbalance in the test-rig that resulted in a slightly uneven load distribution.

10 Crack development

10.1 Crack registration

The crack development was registered for each load step during testing of the beams, but the main registration was done at approximately 50% of maximum load capacity in order to compare with the estimated crack widths and distances in SLS. The crack widths were measured using a binocular and a measuring scale. All the beams had in common that the crack widths were small at this stage, and since the smallest stripe on the scale for comparison was 0,08 mm it was difficult to measure an exact value for smaller crack widths than this. This turned out to be a problem, since most of the crack widths were in fact equal to, or smaller than this value at the relevant load step. At the time of testing, it was assumed that these minor cracks were inconsequential. Estimation of the expected crack widths was first conducted after the testing was finished, and it turned out that some of the beams in fact had expected crack widths smaller than 0,08 mm. With this knowledge in mind, the crack widths should have been more meticulously measured to get a more accurate result for comparison with the estimation. In the following results, the maximum crack width w_{max} and the mean distance between cracks $s_{r,m}$ are shown for the relevant load steps.

10.1.1 Beam series M1

This series had three reinforcement bars, and both the load capacity and the crack development were similar for the two beams. The cracks were nicely distributed along the beam length and the crack widths were small at the 50% load step. The cracks increased in both number and widths as the loading increased, and at the load step just prior to failure the largest crack width was measured to 0,25 mm and 0,60 mm for the two beams respectively.

Beam	Capacity [kN]	Reg. load step [kN]	No. of cracks	w_{max}[mm]	$s_{r,m}$[mm]
M1-1	113,2	54,0	21	0,08	112
M1-2	109,9	54,0	20	0,08	102

Table 16: Crack registration for beam series M1

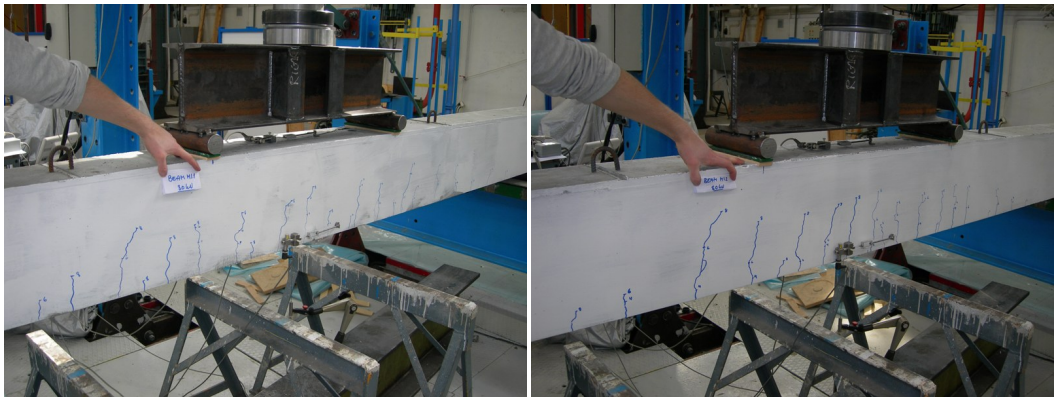

(a) M1-1 (b) M1-2

Figure 43: Cracks beam series M1

10.1.2 Beam series M2

The two beams in series M2 also had a similar moment capacity. However, the crack development at the 50% load step was more extensive for beam M2-1 than M2-2, but at the same time the crack widths were small for both beams. At the load step just before failure, the crack widths had increased to 0,20 mm and 0,30 mm for M2-1 and M2-2 respectively. At this stage, the number of cracks had also evened out between the two beams, with 30 and 34 cracks.

Beam	Capacity [kN]	Reg. load step [kN]	No. of cracks	w_{max}[mm]	$s_{r,m}$[mm]
M2-1	72,7	33,5	18	<0,08	101
M2-2	68,0	33,5	9	<0,08	159

Table 17: Crack registration for beam series M2

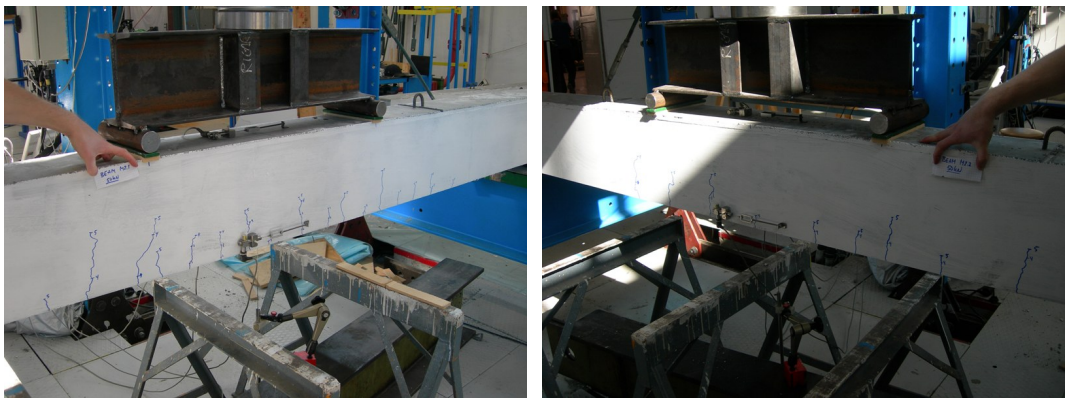

(a) M2-1 (b) M2-2

Figure 44: Cracks beam series M2

10.1.3 Beam series M3

This series had no reinforcement bars, hence the capacity for these beams were lower than the other series. Moreover, this was the series with most spread in capacity for the two beams. The first visible cracks did not occur until approximately 80% of the moment capacity, thus registration of cracks at 50% was not relevant for this series. Both beams were checked at a corrected jack load of 33,5 kN (displayed 50kN due to calibration error). Even just prior to failure, the crack widths remained small and the largest registered crack width was 0,08 mm.

As can be seen from table 18, beam M3-1 reached its maximum load just after the current load step. The substantial difference in capacity results in twice as many cracks in beam M3-1 as beam M3-2 at the same load step.

Beam	Capacity [kN]	Reg. load step [kN]	No. of cracks	w_{max}[mm]	$s_{r,m}$[mm]
M3-1	34,2	33,5	12	0,08	122
M3-2	42,9	33,5	6	0,08	154

Table 18: Crack registration for beam series M3

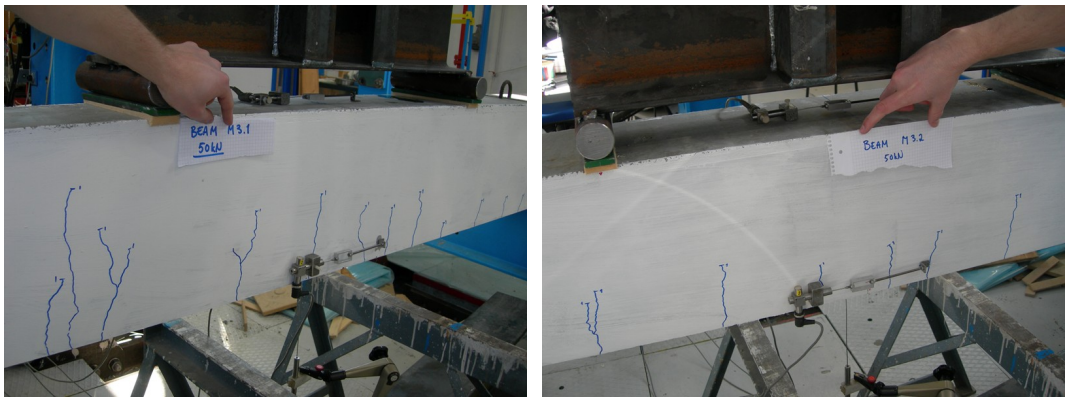

(a) M3-1 (b) M3-2

Figure 45: Cracks beam series M3

The measured crack widths for all of the six beams were very small at the registration load step. Even the beams with only fibre reinforcement had small crack widths and this indicates that the fibres serve their purpose with respect to limiting crack widths. The measured mean crack distances are however different for the two beams in both series M2 and M3. For series M3 this is probably due to the difference in maximum capacity. The reason for the difference in crack development for series M2 is unknown, but it may be because the crack pattern was not yet fully developed at the given load step.

10.2 Estimation of cracks

10.2.1 Calculation parameters

For the two beam series M1 and M2 with both fibres and reinforcement bars, a calculation of estimated crack widths and crack distances was performed after the testing. The formulas used in the calculations are described in chapter 4.1, and are based on the COIN-guidelines and EC2. The formulas are embedded in a service-ability limit state sheet in the multi-layer program in excel, and this program was used for the calculation. An advantage by using this program, is that it calculates 30 strain steps to determine the moment-curvature diagram. Each of these steps includes a computation of the tensile strength in the reinforcement bars σ_s and the compressive zone height αd . Both these parameters are necessary input values to estimate the crack widths and distances, and they can easily be extracted at a given strain state. In the calculations, these values were found at the strain step equivalent to 50% of the moment capacity, since this was the state of which cracks were registered during testing. If the relevant moment state was between two strain steps in the program, linear interpolation was used to find the correct value.

In order to get an estimation closely related to the actual behaviour of the beams, the parameters found in the curve-fitting described in section 9.3.7 were used in the multi-layer method simulations. This meant using an adjusted value for $f_{ftk,res2,5}$, and not the value from testing of standard beams which certainly was too high. In the master thesis of Steinnes, Simpson, Nordhus[10], $f_{ftk,res0,5}$ was suggested used in serviceability instead of $f_{ftk,res2,5}$. However, the COIN-guidelines uses $f_{ftk,res2,5}$ in the formulas, and this was chosen also in this thesis. Since these two values are quite similar in the standard beam results, this choice will not be of major significance.

To assess the fibre effect on cracking, simulations with $f_{ftk,res2,5} = 0$ was performed. Naturally, this lead to a major decrease in the moment capacity compared to the simulation with fibres, thus comparison of crack widths at the same loading would have a major effect. This comparison was only possible to do for the beams with three reinforcement bars, since the beams in series M2 would have failed before the 50% load step in the simulation without fibres. In order to give an indication on the fibre effect also for series M2, σ_s and αd were taken from the state with equal strain ε_{uk} as for the estimation with fibres. In addition, the factor k_5 was set to 1.

10.2.2 Crack widths

Estimation for comparison with test results The material parameters used in the multi-layer method for estimating the crack widths are presented in table 19.

Series	f_{ck}	$f_{ftk,res2,5}$	f_{ctm}
M1	59,0	3,9	4,33
M2	59,0	3,8	4,33

Table 19: Parameters from curve-fitting

These values were used to run the simulation in the excel program. Values for σ_s and αd were then found at 50% of the estimated moment capacity. The strain in the relevant step was also registered, for use in the comparison of fibre effect. This resulted in the following estimated crack widths:

Series	$M_{50\%}$[kNm]	ε_{uk}	σ_s [MPa]	αd [mm]	w_k[mm]
M1	37	0,85‰	142	95	0,04
M2	22,5	0,40‰	66	143	0,02

Table 20: Estimated crack widths

Assessment of fibre effect based on equal strains

Simulations without fibres were conducted at equal strain states as the 50% moment capacity for the simulations with fibres to assess the fibre contribution. In this calculation, $f_{ftk,res2,5} = 0$, and thus the fibre contribution factor $k_5 = 1$. In addition, the compressive zone height at the equal strain state will decrease without the fibre contribution.

Series	ε_{uk}	αd [mm]	w_k[mm]
M1	0,85‰	77	0,06
M2	0,40‰	131	0,05

Table 21: Estimated crack widths without fibre contribution

Assessment of fibre effect based on equal loading For beam series M1, a simulation was performed to see what the crack widths would have been for the same loading if the beams had no fibres. As expected, the estimated crack width was severely increased.

Series	$M_{50\%}$[kNm]	σ_s [MPa]	αd [mm]	w_k[mm]
M1	37	420	57	0,20

Table 22: Fibre effect for equal loading

Discussion The estimated crack widths are smaller than the measured values. These small values make it difficult to assess the exact deviation between the estimated and measured crack widths due to the measuring accuracy. However, the

measured values were slightly higher than the estimation and this indicates that the calculation based on the multi-layer method is not a conservative approach.

The simulation of fibre effect based on equal strains give larger crack widths as can be seen in tables 20 and 21. The fibres increasing effect on the compressive zone αd, has minor effect on the calculated crack widths in the simulation. The main effect on the larger crack widths in the formulas comes from the factor k_5.

The fibre effect based on equal loading in table 22 shows that the total fibre contribution significantly reduces the crack widths compared to a conventionally reinforced beam without fibres. The lack of fibres results in a much higher stress in the reinforcement bars, thus also a higher strain. Consequently, the crack widths will increase.

10.2.3 Crack distance

The mean crack distance $s_{r,m}$ was calculated from the estimated maximum crack distance. The COIN-report suggests using the expression $s_{r,m} = \frac{s_{r,max}}{1,7}$. In the master thesis of Nordhus, Simpson, Steinnes[10], similar moment beams were tested. Here it was found that the expression $s_{r,m} = \frac{s_{r,max}}{1,33}$ derived by Ingemar Löfgren[8], gave an estimation closer to the test results than the expression in the COIN-guidelines. In this thesis, both expressions were checked against the measured distance to study which expression gave the best result. The results are presented in table 23 and also plotted in the diagrams in figure 46 for comparison between the measured and calculated values.

Series	$\frac{s_{r,max}}{1,7}$	$\frac{s_{r,max}}{1,33}$	Measured $s_{r,m}$
M1-1	52	67	112
M1-2	52	67	102
M2-1	68	86	101
M2-2	68	86	159

Table 23: Mean crack distances

The estimated distances do not match the measured distances very well. Both the estimation formulas, $\frac{S_{r,max}}{1,7}$ and $\frac{S_{r,max}}{1,33}$, suggest too low mean crack distances compared to the measured values. The reason for this could be that the crack pattern was not yet fully developed at the given load state. Especially for series M2, the measured mean distance varies significantly between the two beams within the series. At the 50% load step beam M2.1 had twice as many cracks as beam M2.2. A more similar crack pattern developed with further increasing load.

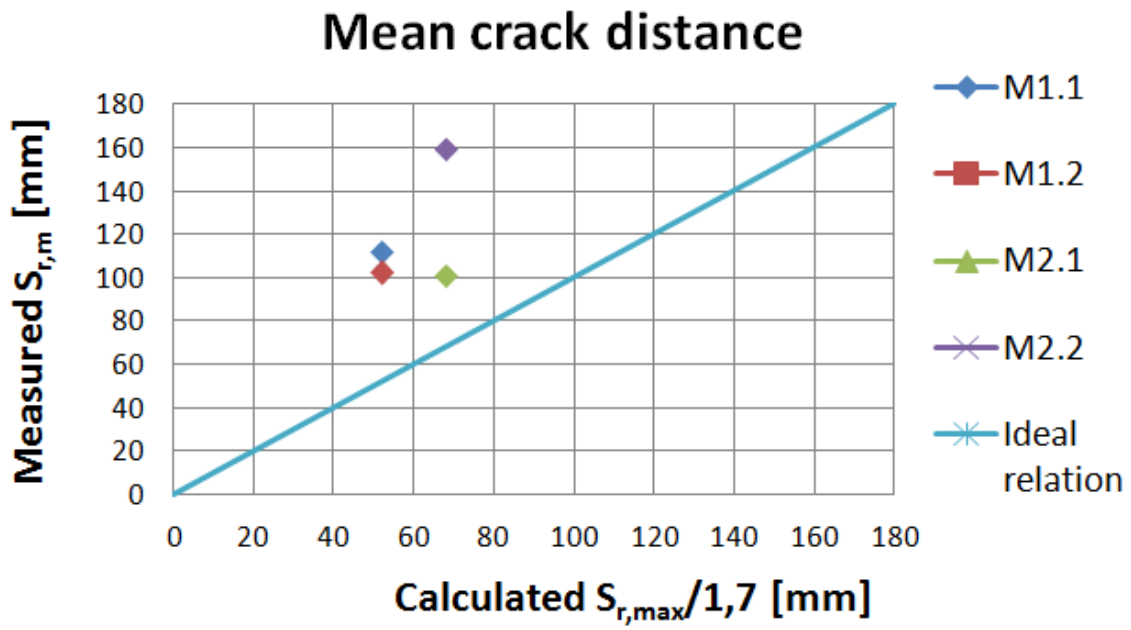

(a) $S_{r,max}/1,7$

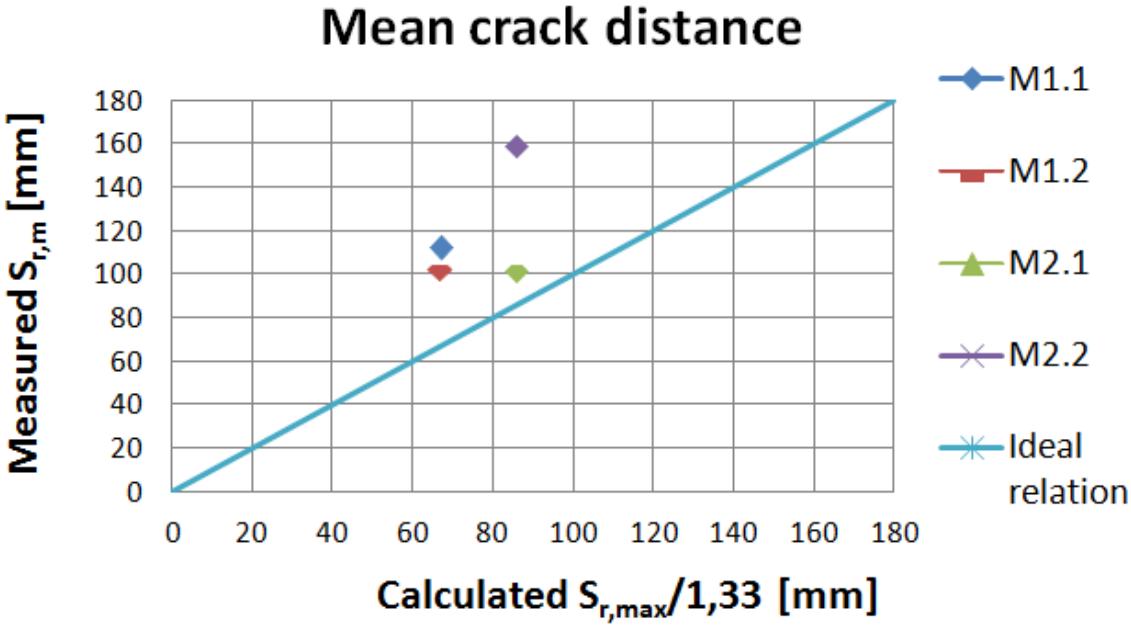

(b) $S_{r,max}/1,33$

Figure 46: Relation between measured and calculated mean crack distances

Fibre effect on crack distance

The two factors that influence the calculations of the crack distance are the fibres increasing effect on the compressive zone and the factor k_5. Considering the fibre effect at equal strain state, there is only a marginal difference in the compressive zone with and without fibres, thus this will have minor effect on the estimated distance. The factor $k_5$will however have major impact on the calculation, due to the high values of $f_{ftk,res2,5}$. The results are presented in the table 24.

Series	$\frac{s_{r,max}}{1,7}$ [mm]	$\frac{s_{r,max}}{1,33}$ [mm]
M1	102	131
M2	170	217

Table 24: Mean crack distances without fibre contribution

As expected, the estimated distance between cracks increases significantly as the fibre contribution is excluded.

10.2.4 Crack moment

The estimated crack moment was also found by using the serviceability sheet in the multi-layer program. For the formulas used in the calculations, the fibres had no influence on the estimated crack moment. This may be because the fibres purpose is to transfer stress when cracks occur, hence they will have minor effect before cracking.

Series	$M_r$with fibres	$M_r$without fibres
M1	14,0	14,0
M2	13,3	13,3

Table 25: Estimated crack moments

The load step where the first visible cracks occurred during testing was used as a rough indication for the crack loading. Also, the load-displacement diagrams for each beam were used. The point on the curve where the linear behaviour ends, is the approximate crack load. This method of finding the crack moment is not very accurate and is only a rough estimate. The results show that the measured and calculated values match quite well.

	M1-1	M1-2	M2-1	M2-2	M3-1	M3-2
$M_{r-measured}$[kNm]	13	16	12	13	10	11

Table 26: Approximate crack moments from testing

10.2.5 Discussion cracks

All of the beams had small crack widths and an even distribution of cracks. The crack development registered at 50 % of maximum capacity was insignificant compared to the demands in serviceability state. EC2 table 7.1N suggests a maximum crack width of 0,4 mm, and all of the measured crack widths are much smaller than this.

When comparing at the estimated crack widths and crack distances, the estimation suggested a more favourable crack distribution than what was actually measured. The formulas suggested both smaller crack widths and crack distances. This was not a conservative estimation since a crack distribution with many small cracks is desirable instead of fewer, but larger cracks. Still, the crack development observed during testing was satisfactory and within the requirements in serviceability.

A disadvantage in the testing with respect to cracking, was that no beams without fibres were cast. As a result of this, the crack development without fibres could not be found based on the testing, but had to be simulated based on the formulas in COIN and EC2. Nevertheless, all of the simulations showed that the fibres had a beneficial effect on both crack widths and crack distances.

11 Comments on the results and suggestions for further work

An interesting element in the test results was that the main failure crack in five out of six beams occurred at the same point along the beam length. The main crack developed on the same side as the beams were cast from. The assumption that the failure occurred because the flow in the concrete transported more fibres away form the casting point, needs more investigation to be confirmed. If the assumption is valid, this needs to be taken account for in design of self compacting fibre reinforced concrete beams.

The fibres contribution to the tensile strength $f_{ftk,res2,5}$ was found to be larger in the test beams with bar reinforcement than for the beams with only fibres. A possible reason could be that bar reinforcement give fibres a more favourable orientation during casting. When self compacting concrete is cast from one end of the beam and flows along the direction of the bar reinforcement, it could make the fibres align parallel to the bars. This assumption needs more investigation to be supported.

When the cracks in the beams were examined, the relation between the estimated values and the test measurements did not match very well. The crack widths measured were small and hard to measure, but the result showed that the estimated values were smaller than the measured values. One of the reasons for this result could be that the crack pattern was not fully developed at the state of registration, but further tests should be performed to investigate if the current calculation methods are appropriate also for small crack widths.

Part V

Conclusion

This conclusion is based on observed behaviour of six fibre reinforced beams in a 4-point bending test. Two of the beams were only fibre reinforced, while four had additional reinforcement bars.

The fibres contribution to the moment capacity was represented with a residual tensile strength $f_{ftk,res2,5}$ according to the current guidelines by COIN. In testing, all of the beams had substantially higher moment capacity than calculated in the design. The results from testing of standard beams suggested an even higher residual tensile strength than what was found from the large beam testing. In any case, it can be concluded that the fibre contribution was greater than assumed before testing.

The residual tensile strength from the fibres was found to have a greater influence on the moment capacity in the beams with additional reinforcement bars compared to the beams with only fibre reinforcement. Still, it should be mentioned that the two beams with only fibre reinforcement had a significant difference in total moment capacity, thus the exact fibre contribution in these two beams was difficult to assess. Due to the limited number of tested beams it is hard to draw an absolute conclusion on this.

All the beams showed a ductile failure behaviour. The beams with only fibre reinforcement did also sustain capacity to some extent after maximum load was reached, confirming that fibre reinforced beams can be designed without additional rebars and still satisfy the demands to ductile behaviour. The test results also showed that the load capacity increased after cracking, hence hardening behaviour was satisfied. This shows that it is possible to meet the requirements to minimum reinforcement by using only fibre reinforcement as suggested in the COIN-guidelines.

The registered crack development at 50% of maximum load capacity was not extensive. The measured crack widths were much smaller than the demands in serviceability state and the cracks were evenly distributed. Since no beams without fibre reinforcement were tested, the fibre contribution could only be estimated by comparing with calculated values. The calculation of estimated crack widths and crack distances did not match the measured values perfectly, but the simulations unambiguously suggested that the fibres had a beneficial contribution to limit cracking.

References

[1] Norsk Betongforening. Nb publikasjon nr. 29: Spesifikasjon og produksjonsveiledning for selvkomprimerende betong. Technical report, 2007.

[2] Norsk Betongforening. Nb publikasjon nr. 7: Sprøytebetong til bergsikring. Technical report, 2011.

[3] COIN. Ligthweight aggregate concrete - improvement of ductility by using fibre reinforcement (draft). Technical report, 2012.

[4] COIN. State of the art - ultra high performance fibre reinforced concrete (draft). Technical report, 2012.

[5] Terje Kanstad et al. COIN. Coin project report 29: Forslag til retningslinjer for dimensjonering, utførelse og kontroll av fiberarmerte betong. Technical report, SINTEF, NTNU, 2011.

[6] Bill Mosley et al. *Reinforced Concrete Design - to eurocode 2.* Palgrave macmillan, 2007.

[7] Pål Gjerp, Morten Opsahl, and Sverre Smeplass. *Grunnleggende betongteknologi.* Byggenæringens forlag, 2004.

[8] Ingemar Löfgren. Caculation of crack width and crack spacing, workshop. Technical report, 2007.

[9] Magne Maage. *Concrete Technology 1 - Chapter 1 - Practice.* NTNU, 2008.

[10] Steinnes Nordhus, Simpson. Fiberarmerte betongkonstruksjoner. Master's thesis, The Norwegian Inst. of Technology, 2011.

[11] Standard Norge. Eurokode2: Prosjektering av betongkonstruksjoner. Del 1-1: Allmenne regler og regler for bygninger .

[12] Standard Norge. NS-EN 14651: Test method for metallic fibre concrete-Measuring the flexural tensile strength.

[13] Standard Norge. NS-EN 14889-1: Fibres for concrete - Part 1: Steel fibres.

[14] Standard Norge. NS-EN 14889-2: Fibres for concrete - Part 2: Polymer fibres.

[15] Nicolas Roussel. Correlation between yield stress and slump: Comparison between numerical simulations and concrete rheometers results. Technical report, LCPC, France, 2005.

[16] Nicolas Roussel. The lcpc box: a cheap and simple technique for yield stress measurements of scc. Technical report, LCPC, France, 2005.

[17] Åse Døssland. *Fibre reinforcement in load carrying concrete structures.* PhD thesis, The Norwegian Inst. of Technology, 2008.

[18] Sverre Smeplass. *Concrete Technology 1 - Chapter 3 - Fresh concrete-workability.* NTNU, 2004.

[19] Svein Ivar Sørensen. *Betonkonstruksjoner - Beregning og dimensjonering etter Eurocode 2.* Tapir akademisk forlag, 2010.

[20] Lars Thrane, Claus Pade, and Claus Nilsen. Determination of rheology of self-consolidating concrete using the 4c-rheometer and how to make use of the results. Technical report, DTI, Denmark, 2008.

[21] Lucie Vandewalle. Fibre reinforced concrete and the new fib model code. *WORKSHOP Fibre reinforced concrete Trondheim Nov. 2007*, pages 5–12.

Appendix

1 - Moment calculations

2 - Anchoring calculations

3 - Displacement-curvature relation

4 - Concrete recipe

Appendix 1

Simplified method for moment capacity

Input data

$\gamma_c := 1.0$ $\gamma_s := 1.0$

Concrete B35

$f_{ck} := 35MPa$ $f_{cd} := \frac{f_{ck}}{\gamma_c}$

$f_{ctm} := 3.2MPa$

$f_{cteff} := f_{ctm}$

$\varepsilon_{cu3} := 0.0035$

$c := 25mm$

Reinforcement bars

$f_{yk} := 500MPa$ $f_{yd} := \frac{f_{yk}}{\gamma_s}$

$E_s := 200000MPa$

$\varepsilon_{yk} := 0.0025$ $\varepsilon_{yd} := \frac{\varepsilon_{yk}}{\gamma_s}$

$\varepsilon_{ud} := 0.030$

$Ø := 12mm$

Fibre reinforcement

$f_{ftk.res2.5} := 2MPa$ $f_{ftd.res2.5} := \frac{f_{ftk.res2.5}}{\gamma_c}$

Cross sectional data

$b := 200mm$

$h := 300mm$

$d_2 := h - c - \frac{1}{2}Ø$ $d_3 := h - c - Ø$

Moment capacity for beam with no bar reinforcement

$$M_{Rd1} := 0.4 \cdot f_{ftd.res2.5} \cdot b \cdot h^2$$

$$P_{Rd1} := \frac{M_{Rd1}}{0.65m}$$

$M_{Rd1} = 14.4 \cdot kNm$ $P_{Rd1} = 22.154 \cdot kN$

Minimum required bar reinforcement

Coin project report

$$A_{smin1} := \frac{0.26 \cdot b \cdot d_2 \cdot \left(f_{ctm} - 2.1 \cdot f_{ftk.res2.5} \right)}{f_{yk}} = -27.976 \cdot mm^2$$

$$A_{smin2} := 0.0013 \cdot b \cdot d_2 \cdot \left(1 - \frac{2.1 \cdot f_{ftk.res2.5}}{f_{ctm}} \right) = -21.856 \cdot mm^2$$

$$A_{smin} := \max\left(A_{smin1}, A_{smin2} \right) = -21.856 \cdot mm^2$$

No need for bar reinforcement when the fibre contribution are included in the minimum reinforcement calculation

EC2

$$A_{smin} := 0.26 \cdot b \cdot d_2 \cdot \frac{f_{ctm}}{f_{yk}} = 89.523 \cdot mm^2 \qquad A_{smin} = 89.523 \cdot mm^2$$

Cross section capacity with minimum reqiured bar reinforcement

Using one 12 mm bar

$n_2 := 1$ $\quad d_2 = 269 \cdot mm$

$A_{s2} := n_2 \cdot \pi \cdot \left(\frac{Ø}{2}\right)^2$ $\quad A_{s2} = 113.097 \cdot mm^2$

Equilibrium formulas

$T_c = S_f + S_a$ $\quad T_c = 0.8 \cdot x \cdot b \cdot f_{ck}$

$S_f = (h - x) \cdot b \cdot f_{ftk.res2.5}$ $\quad S_a = A_s \cdot f_{yk}$

Compression zone height

$$x_2 := \frac{A_{s2} \cdot f_{yd} + h \cdot b \cdot f_{ftd.res2.5}}{0.8 \cdot b \cdot f_{cd} + b \cdot f_{ftd.res2.5}}$$ $\quad x_2 = 29.425 \cdot mm$

Reinforcement strain control

$\alpha_2 := \frac{x_2}{d_2}$ $\quad \alpha_2 = 0.109$

$\varepsilon_{s.2} := \frac{1 - \alpha_2}{\alpha_2} \cdot \varepsilon_{cu3}$ $\quad \varepsilon_{s.2} = 0.028$

$\varepsilon_{s.2} < \varepsilon_{ud}$

Moment capacity

$T_{c2} := 0.8 \cdot x_2 \cdot b \cdot f_{cd}$ $\quad T_{c2} = 164.779 \cdot kN$

$S_{a2} := A_{s2} \cdot f_{yd}$ $\quad S_{a2} = 56.549 \cdot kN$

$S_{f2} := \left(h - x_2\right) \cdot b \cdot f_{ftd.res2.5}$ $\quad S_{f2} = 108.23 \cdot kN$

$M_{Rd2} := S_{f2} \cdot \left(0.5 \cdot h - 0.1 \cdot x_2\right) + S_{a2} \cdot \left(d_2 - 0.4 x_2\right)$

$P_{Rd2} := \dfrac{M_{Rd2}}{0.65m}$

$M_{Rd2} = 30.462 \cdot kNm$ $\quad P_{Rd2} = 46.865 \cdot kN$

Shear control

$k_1 := 0.15$ $k_2 := 0.15$ $f_{ck.v} := 35$

$C_{Rd.c} := \frac{k_2}{\gamma_c}$ $\rho_{l.2} := \min\left(0.02, \frac{A_{s2}}{b \cdot d_2}\right)$

$\sigma_{cp} := 0MPa$ $k := \min\left(2, 1 + \sqrt{\frac{200mm}{d_2}}\right)$

$$V_{Rd.ct2} := \left[C_{Rd.c} \cdot k \cdot \left(100 \cdot \rho_{l.2} \cdot f_{ck.v}\right)^{\frac{1}{3}} + k_1 \cdot \sigma_{cp}\right] \cdot b \cdot d_2 \cdot \frac{N}{mm^2}$$

$V_{Rd.cf2} := 0.6 \cdot f_{ftk.res2.5} \cdot b \cdot h$ $V_{Rd.cf2} = 72 \cdot kN$

$V_{Rdc2} := V_{Rd.ct2} + V_{Rd.cf2}$

$P_{Rdv2} := V_{Rdc2} \cdot 2$

$P_{Rdv2} = 202.46 \cdot kN$

Cross sectional capacity with 3 times minimum required reinforcement area

$n_3 := 3$ $\qquad$ $d_3 = 263 \cdot mm$

$A_{s3} := n_3 \cdot \pi \cdot \left(\frac{Ø}{2}\right)^2$ $\qquad$ $A_{s3} = 339.292 \cdot mm^2$

Reinforcement condition

$\alpha_{bal} := \frac{\varepsilon_{cu3}}{\varepsilon_{cu3} + \varepsilon_{yd}}$ $\qquad$ $\alpha_{bal} = 0.583$

$A_{sb} := \frac{\alpha_{bal} \cdot 0.8 \cdot d_3 \cdot b \cdot f_{cd} - \left(h - \alpha_{bal} \cdot d_3\right) \cdot b \cdot f_{ftd.res2.5}}{f_{yd}}$

$A_{sb} = 1601 \cdot mm^2$

$A_s < A_{sb}$

The cross section is under reinforced

Compression zone height

$x_3 := \frac{A_{s3} \cdot f_{yk} + h \cdot b \cdot f_{ftk.res2.5}}{0.8 \cdot b \cdot f_{ck} + b \cdot f_{ftk.res2.5}}$ $\qquad$ $x_3 = 48.274 \cdot mm$

Reinforcement strain control

$\alpha_3 := \frac{x_3}{d_3}$ $\qquad$ $\alpha_3 = 0.184$

$\varepsilon_{s3} := \frac{1 - \alpha_3}{\alpha_3} \cdot \varepsilon_{cu3}$ $\qquad$ $\varepsilon_{s3} = 0.016$

$\varepsilon_{s3} < \varepsilon_{ud}$

Moment capacity

$T_{c3} := 0.8 \cdot x_3 \cdot b \cdot f_{ck}$ $\quad T_{c3} = 270.336 \cdot kN$

$S_{a3} := A_{s3} \cdot f_{yk}$ $\quad S_{a3} = 169.646 \cdot kN$

$S_{f3} := \left(h - x_3\right) \cdot b \cdot f_{ftk.res2.5}$ $\quad S_{f3} = 100.69 \cdot kN$

$M_{Rd3} := S_{f3} \cdot \left(0.5 \cdot h - 0.1 \cdot x_3\right) + S_{a3} \cdot \left(d_3 - 0.4 x_3\right)$

$P_{Rd3} := \dfrac{M_{Rd3}}{0.65m}$

$M_{Rd3} = 55.959 \cdot kNm$ $\quad P_{Rd3} = 86.09 \cdot kN$

Shear control

$$\rho_{l.3} := \min\left(0.02, \frac{A_{s3}}{b \cdot d_3}\right) \qquad \underset{\sim}{k} := \min\left(2, 1 + \sqrt{\frac{200mm}{d_3}}\right)$$

$$V_{Rd.ct3} := \left[C_{Rd.c} \cdot k \cdot \left(100 \cdot \rho_{l.3} \cdot f_{ck.v}\right)^{\frac{1}{3}} + k_1 \cdot \sigma_{cp}\right] \cdot b \cdot d_3 \cdot \frac{N}{mm^2}$$

$$V_{Rd.cf3} := 0.6 \cdot f_{ftk.res2.5} \cdot b \cdot h$$

$$V_{Rdc3} := V_{Rd.ct3} + V_{Rd.cf3}$$

$$P_{Rdv3} := V_{Rdc3} \cdot 2$$

$$P_{Rdv3} = 227.491 \cdot kN$$

Appendix 2

Anchoring length according to EC2

$\gamma_c := 1.0$ $\quad$ $\text{Ø} := 12\text{mm}$

Available anchoring length $\quad$ 300mm

Beam series M2 - 1 Ø 12

Design failure load $\quad$ $P_{Rd} := 47.6\text{kN}$

Max shear force: $\quad$ $V_{Ed} := \frac{P_{Rd}}{2} = 23.8\cdot\text{kN}$

Sress in bar reinforcement:

Assume $\quad$ $\theta := 45\cdot\text{deg}$

$\Delta F_{td} := V_{Ed}\cdot\cot(\theta)$ $\quad$ $\Delta F_{td} = 23.8\cdot\text{kN}$

$\sigma_{sd} := \frac{\Delta F_{td}}{113\text{mm}^2}$ $\quad$ $\sigma_{sd} = 210.619\cdot\text{MPa}$

[8.4.2] Bonding

$f_{ctk.0.05} := 2.2\text{MPa}$

$\eta_1 := 1.0$

$\eta_2 := 1.0$

$f_{ctd} := \frac{f_{ctk.0.05}\cdot 0.85}{\gamma_c}$ $\quad$ $f_{ctd} = 1.87\cdot\text{MPa}$

$f_{bd} := 2.25\cdot\eta_1\cdot\eta_2\cdot f_{ctd}$ $\quad$ $f_{bd} = 4.207\cdot\text{MPa}$

[8.4.3] Force introduction length

$$l_{b.rqd} := \frac{Ø}{4} \cdot \frac{\sigma_{sd}}{f_{bd}} \qquad l_{b.rqd} = 150.174 \cdot mm$$

[8.4.4] Anchoring length

$$l_{bd} := \max\left(l_{b.rqd}, 10 \cdot Ø, 100mm\right) \qquad l_{bd} = 150.174 \cdot mm$$

$$l_{bd} < 300mm$$

Beam series M1 - 3 Ø 12

Design failure load: $P_{Rd2} := 87.6kN$

Max shear force: $V_{Ed2} := \frac{P_{Rd2}}{2} = 43.8 \cdot kN$

Sress in bar reinforcement:

$$\Delta F_{td2} := V_{Ed2} \cdot \cot(\theta) \qquad \Delta F_{td2} = 43.8 \cdot kN$$

$$\sigma_{sd2} := \frac{\Delta F_{td2}}{3 \cdot 113mm^2} \qquad \sigma_{sd2} = 129.204 \cdot MPa$$

[8.4.2] Bonding

$f_{ctk.0.05} = 2.2 \cdot MPa$

$\eta_1 = 1$

$\eta_2 = 1$

$f_{ctd} = 1.87 \cdot MPa$

$f_{bd} = 4.207 \cdot MPa$

[8.4.3] Force introduction length

[8.9.1] Bundled reinforcement

$\varnothing_n := 12mm$ $\quad$ $n_b := 3$

$\varnothing_b := \varnothing_n \cdot \sqrt{n_b}$ $\quad$ $\varnothing_b = 20.785 \cdot mm$

$l_{b.rqd2} := \frac{\varnothing_b}{4} \cdot \frac{\sigma_{sd2}}{f_{bd}}$ $\quad$ $l_{b.rqd2} = 159.563 \cdot mm$

[8.4.4] Anchoring length

$l_{bd2} := \max\left(l_{b.rqd2}, 10 \cdot \varnothing_b, 100mm\right)$ $\quad$ $l_{bd2} = 207.846 \cdot mm$

$l_{bd2} < 300mm$

Appendix 3

Displacement-curvature relation

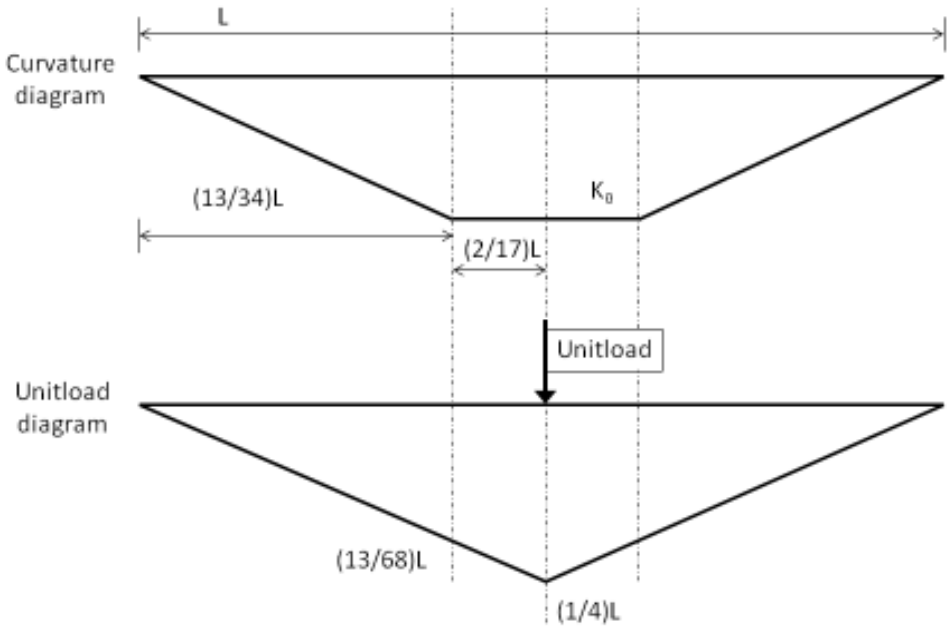

$$\delta = \int_{L}^{0} \kappa(x) \cdot M(x)\, dx$$

Solving the integral by speed integration tables.

$$\delta = 2 \cdot \left[\frac{1}{3} \cdot \kappa_0 \cdot \frac{13}{68} \cdot L \cdot \frac{13}{34} \cdot L + \frac{1}{2} \cdot \kappa_0 \cdot \left(\frac{1}{4} \cdot L + \frac{13}{68} \cdot L \right) \cdot \frac{2}{17} \cdot L \right]$$

$$\delta = \frac{349}{3468} \cdot \kappa_0 \cdot L^2$$

$$\kappa = \frac{3468}{349} \cdot \frac{\delta}{L^2}$$

Extra Water
Mix gives to NTNU

Laboratorieprotokoll

unicon
CEMENTIR HOLDING

Produksjons-ID	2012031310026	Protokoll type	Sats
Blandetidspunkt	13.03.2012 09:44:16	Tømmetid	09:53:11
Resept	UN53A-D103	B30 M60 16mm SKB	
Blander	M1	Satsstørrelse	1,80 m³
		Satsnummer	1
Miljøklasse	M60	Produsert konsistens	260
Ordrenummer	0000474469	Følgeseddelnummer	1892963
Kunde	0001014413	Unicon AS (region midt)	
Plass	NTNU	Høgskoleringen 1	
Bil	857	Bilregistereingsnummer	VT14311

Iaterial	Enhet	Fukt %	Resept	Bør	Er	Alarm	Avvik	%	Er kg/m³	VOT kg/m³	Vann kg/m³	Dens.	VOT l/m³
Norcem Std-FA Kjøps	kg		393	708	710		2	0,3	390,5	390,5	0,0	3010	129,7
Flyveaske k=0,7	kg		85	152	150		-2	-1,3	82,5	82,5	0,0	2200	37,5
Silika ikke med i V/C	kg		18,1	32,6	32,4		-0,2	-0,6	17,8	17,8	0,0	2200	8,1
0-8 Forset	kg	4,5	1300	2445	2424		-21	-0,9	1333,3	1275,9	57,4	2700	472,6
8-16mm Vassfjell	kg	0,2	366	660	666		6	0,9	366,3	365,6	0,7	3040	120,3
Glenium SKY 600	kg	82,0	4,72	8,50	8,44		-0,06	-0,7	4,6	0,8	3,8	1193	0,7
Kaldt vann	kg		136	138	138		0	0,0	75,9	0,0	75,9	1000	0,0
Varmt vann	kg		50	90	90		0	0,0	49,5	0,0	49,5	1000	0,0
Dramix Ready	kg		80,00	144,00	144,00		0,00	0,0	79,2	79,2	0,0	7850	10,1
Ekstra vand	ltr		0	0	25		25	0,0	13,8	0,0	13,8	1000	0,0
Total	kg		2432,5	4378,1	4387,8				2413,6	2212,4	201,1		779,0

	Resept	Bør	Er	Enhet	Avvik	%	l/m³
VOT		1422,0	1416,2	l	-5,8	-0,4	779,0
Luft (2,0 %)	20,0	36,0	36,4	l	0,4	1,0	20,0
Tilsat vand		228,0	253,0	l	25,0	11,0	139,2
Total fugt		113,6	112,6	l	-0,9	-0,8	62,0
Total		1800,0	1818,0	l	18,0	1,0	1000,1
V/C	0,420	0,420	0,449		0,029	6,9	
Total vand/pulver tal		0,380	0,410		0,030	7,9	
Maks. vand	195	350		kg			
Vann/betong		7,8	8,3	%	0,5	6,8	
Total blandetid	60	60	292	Sek.	232	386,7	
Slutblandetid	10	10	11	Sek.	1	10,0	
Temperatur		20,0	19,7	°C	-0,3	-1,7	
Wattmeter (tabel)		73	141		68	93,2	
Wattmeter tomgang og sluttverdi		-29	105				
Chlorid	0,06	0,06	0,06	% av pulver	0,00	0,0	
Mørtelindhold	398,00	716,00	740,00	l	24,00	3,4	
Fillerindhold	576,71	1038,13	1037,92	kg	-0,21	0,0	